

**METHANOL PERMEATION THROUGH
PROTON EXCHANGE MEMBRANES OF DIRECT
METHANOL FUEL CELLS**

BY

Mukhtar Bello

A Thesis Presented to the
DEANSHIP OF GRADUATE STUDIES

KING FAHD UNIVERSITY OF PETROLEUM & MINERALS

DHAHRAN, SAUDI ARABIA

In Partial Fulfillment of the
Requirements for the Degree of

MASTER OF SCIENCE

In

Chemical Engineering

May 2006

KING FAHD UNIVERSITY OF PETROLEUM & MINERALS
DHAHRAN, SAUDI ARABIA

DEANSHIP OF GRADUATE STUDIES

This thesis, written by Mukhtar Bello under the direction of his thesis advisor and approved by his thesis committee, has been presented to and accepted by the Dean of Graduate Studies, in partial fulfillment of the requirements for the degree of MASTER OF SCIENCE IN CHEMICAL ENGINEERING.

Thesis Committee



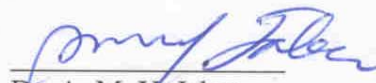
Dr. S. U. Rahman
(Thesis Advisor)



Dr. S. M. J. Zaidi
(Co-advisor)



Dr. Mohammed B. Amin
(Department Chairman)



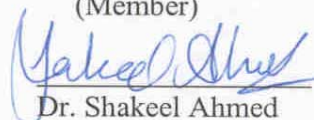
Dr. A. M. Y. Jaber
(Member)



Dr. Mohammed A. Al-Ohali
(Dean of Graduate Studies)



Dr. M. A. Al-Shalabi
(Member)



Dr. Shakeel Ahmed
(Member)

May 28, 2006
Date



DEDICATION

This work is dedicated to my beloved grandmother Mutti.

ACKNOWLEDGEMENT

In the name of Allah, the most beneficent, the most merciful

All praises are due to Allah (SWT) for His guidance and continuous support for me. May the peace and blessings of Allah be upon His noble prophet, Muhammad, his household and companions.

I wish to express my appreciation to Ahmadu Bello University, Zaria, Nigeria, for awarding me a study fellowship and King Fahd University of Petroleum & Minerals, Dhahran, Saudi Arabia for providing the necessary facilities and support for my studies. Also, I am grateful to the Faculty members, Staff, and Technicians of the Chemical Engineering Department, King Fahd University of Petroleum & Minerals for their support.

With deep sense of gratitude, I would like to express my appreciation to my thesis committee members; Dr. S. U. Rahman, Dr. S.M.J. Zaidi, Dr. A. M. Y. Jaber, Dr. M. A. Al-Shalabi, Dr. T. Inui and Dr. S. Ahmed for their immense contributions and support throughout the course of my work. I particularly wish to thank the chairman of the committee, Dr. S.U. Rahman for his excellent cooperation, friendliness, and unlimited accessibility. Special thanks to the laboratory staff; Mr. Mahdi, Mr. Ibrahim, Mr. Kamal, Mr. Mofiz, Mr. Mariano, Mr. Romeo, Mr. Vick (Central Workshop), Mr. Farooq (glass blower, Chemistry Dept.) and Mr. Abdul-Rashid (Research Institute) for their assistance in fabricating some equipment and general services during the experimental work.

My thanks to all the chemical engineering graduate students, especially, Mr. Saidu Muhammad Waziri, Mr. Mohamed Aminuddin, Mr. Suleiman Awwal, Mr. Issam Amr, Mr. Sumon Kazi, and Mr. Hassan Arshad, for their useful suggestions and contributions. Also, I highly appreciate the good relationship and support of the Nigerian Community in Dhahran/Damman. Special thanks to Dr. Nasir Muhammad Tukur, Chairman of Jalsa Group, for his help, useful advises and friendliness from the time of making admission application enquiries till now.

Finally, special thanks to all my relatives and friends for patiently enduring missing me among them, especially my beloved grandmother Mutti.

TABLE OF CONTENTS

DEDICATION	iii
ACKNOWLEDGEMENT	iv
TABLE OF CONTENTS	v
LIST OF TABLES	vii
LIST OF FIGURES	viii
ABSTRACT	x
CHAPTER 1	1
1 INTRODUCTION	1
1.1 Objectives	5
CHAPTER 2	6
2 LITERATURE REVIEW	6
2.1 Fuel Cells	6
2.1.1 Types of Fuel Cells	6
2.1.2 Direct Methanol Fuel Cells (DMFC)	8
2.2 Nafion® membranes Modification	11
2.2.1 Nafion/Organic Blend Membranes	12
2.2.2 Nafion/Inorganic Blend Membranes	13
2.3 Alternative Membranes	15
2.3.1 Sulfonated Poly Ether Ether Ketone (SPEEK) Membranes	15
2.3.2 SPEEK Composite Membranes	17
2.3.3 Sulfonated Poly-Styrene Membranes (SPS)	21
2.3.4 SPS/PTFE Composite Membranes	22
2.3.5 Poly (Vinylidene) Fluoride (PVdF) Composite Membranes	24
2.3.6 Poly-Ethylene Tetrafluoroethylene -based Membranes	24
2.3.7 Polyphosphazene-based Membranes	25
2.3.8 Polyvinyl alcohol/mordenite	25
2.4 Improved Electro oxidation Catalysts	26
2.5 Methanol Crossover Measurement Techniques	27
2.5.1 Monitoring CO ₂ from cathode of DMFC	28
2.5.2 Open Circuit Voltage (OCV)	30
2.5.3 Limiting Current Measurements	32
2.5.4 Gas Chromatography (GC)	33
2.5.5 Mass Spectrometry	34
2.5.6 Cyclic voltammetry and chronoamperometry	35
2.5.7 Potentiometric Technique	37
2.6 Working Electrode Positioning	39
CHAPTER 3	40

3 EXPERIMENTAL SET-UP AND PROCEDURE	40
3.1 Methanol Permeability Determination.....	40
3.1.1 Cell Design and Experimental Set-up.....	40
3.1.2 Procedure for Cyclic Voltammetry	43
3.1.3 Procedure for Chronoamperometry	44
3.1.4 Procedure for Potentiometric Technique	44
3.2 Composite Membranes Preparation.....	45
3.2.1 Loading of Tungstonphosphoric acid onto MCM-41 and Y-zeolite	45
3.2.2 Membranes Preparation	46
3.3 Determination of Methanol Permeability of the SPEEK/TPA/ MCM-41 or Y-zeolite Composite Membranes.....	46
CHAPTER 4	47
4 RESULTS AND DISCUSSION	47
4.1 Determination of Methanol Permeability of Nafion® 117 Membrane.....	47
4.1.1 Cyclic Voltammetry	50
4.1.2 Chronoamperometry	59
4.1.3 Potentiometric Technique	65
4.2 SPEEK/TPA/ MCM-41 or Y-zeolite Composite Membranes Preparation.....	72
4.3 Methanol Permeability of SPEEK/TPA/ MCM-41 Composite Membranes	73
4.4 Methanol Permeability of SPEEK/TPA/ Y-zeolite Composite Membranes	82
CHAPTER 5	91
5 CONCLUSIONS AND RECOMMENDATIONS	91
5.1 Conclusions.....	91
5.2 Recommendations.....	93
REFERENCES	94

LIST OF TABLES

Table	Title	Page
Table 2-1:	Types of Fuel Cells.....	7
Table 4-1:	Flux values for Nafion [®] 117 membrane at various time periods for 2.5M initial methanol concentration.....	70
Table 4-2:	Nafion [®] Membrane Methanol Permeability	71
Table 4-3:	Flux values for 30% (50%MCM-41 and 50% TPA) and 70% SPEEK composite membrane at various times for 2.5M initial methanol concentration.....	76
Table 4-4:	SPEEK/TPA/MCM-41 Membranes Permeability and Flux Values.	81
Table 4-5:	Flux values for 40wt % (60wt %Y-zeolite and 40wt % TPA) and 60wt% SPEEK composite membrane at various times for 2.5M initial methanol concentration.....	85
Table 4-6:	SPEEK/TPA/Y-zeolite Membranes Permeability and Flux Values.....	89

LIST OF FIGURES

Figure	Title	Page
Figure 2-1:	Schematic diagram of a DMFC	9
Figure 2-2:	Chemical Structure of Nafion.	12
Figure 2-3:	Schematic representation of the microstructure of Nafion and SPEEK.	16
Figure 2-4:	Effects of different HPAs on the conductivity of composite membranes as a function of temperature (70% DS).....	18
Figure 2-5:	Methanol permeability in Nafion [®] 115 and composite membranes.	20
Figure 2-6:	Comparison of the Φ (S/cm) parameter of Nafion and the SPS/PTFE composite membranes.....	23
Figure 2-7:	Schematic diagram of DMFC showing CO ₂ crossover	29
Figure 2-8:	OCV as a function of the cathode pressure for Nafion 115 membrane at different DMFC operation times. The dotted lines correspond to the model equation; (o) first measurement; (●) second measurement; (□) third measurement.....	31
Figure 2-9:	Permeability curves at various concentrations.....	36
Figure 2-10:	Variation of (dE/dt) during CH ₃ OH crossover.....	38
Figure 3-1:	Schematic Diagram of the Fabricated Cell	41
Figure 3-2:	Experimental Set-up.....	42
Figure 4-1:	Schematic of methanol crossover through a membrane from reservoir compartment (A) to receiving compartment (B).	48
Figure 4-2:	cyclic voltammograms at a scan rate of 100mV/s for different methanol concentrations.	52
Figure 4-3:	Calibration curve for the cyclic voltammetry.	53
Figure 4-4:	Cyclic voltammograms at a scan rate of 100mV/s for the reservoir compartment (side A) at different time for 2.5M initial methanol concentration. ...	55
Figure 4-5:	Plot of concentration model equation vs. time for an initial methanol concentration of 2.5M.....	57
Figure 4-6:	Cyclic voltammograms at different scan rates after 6 hrs for the receiving compartment (Side B) for 2.5M initial methanol concentration in the reservoir compartment.	58
Figure 4-7:	Chronoamperometric curves for the methanol oxidation at 0.65V vs. SCE for different concentrations.	60
Figure 4-8:	Calibration curve for the chronoamperometry.....	61
Figure 4-9:	Chronoamperometry curves at 0.65V vs. SCE for the receiving compartment (side B) at different time for 2.5M initial methanol concentration.....	63

Figure 4-10: Chronoamperometry curves for both the reservoir compartment (side A) and the receiving compartment (side B) at different time for 2.5M initial concentration.	63
Figure 4-11: Plot of concentration model equation vs. time for an initial methanol concentration of 2.5M.	64
Figure 4-12: Calibration for the Potentiometry.	67
Figure 4-13: Potentiometric curves for the receiving compartment for different initial methanol concentration in the reservoir compartment.	69
Figure 4-14: Methanol concentrations in the receiving compartment during crossover for different initial methanol concentrations in the reservoir compartment.	69
Figure 4-15: Potentiometric curves for pure SPEEK 1.6 membrane and three different SPEEK/TPA/MCM-41 composite membranes.	74
Figure 4-16: Variation in methanol concentration in the receiving compartment for 30wt % (50wt %MCM-41 + 50wt % TPA) and 70wt % SPEEK composite membrane for 2.5M initial methanol concentration in the reservoir compartment.	75
Figure 4-17: Variation in methanol concentration in the receiving compartment for pure SPEEK 1.6 membrane and the SPEEK/MCM-41/TPA composite membranes for 2.5M initial methanol concentration in the reservoir compartment.	78
Figure 4-18: Methanol crossover flux for the pure SPEEK 1.6 membrane and the SPEEK/MCM-41/TPA composite membranes for 2.5M initial methanol concentration in the reservoir compartment.	80
Figure 4-19: Potentiometric curves for pure SPEEK 1.6 membrane and three different SPEEK/TPA/Y-zeolite composite membranes.	83
Figure 4-20: Variation in methanol concentration in the receiving compartment for 40wt % (60wt %Y-zeolite + 40wt % TPA) and 60wt % SPEEK composite membrane for 2.5M initial methanol concentration in the reservoir compartment.	84
Figure 4-21: Variation in methanol concentration in the receiving compartment for the pure SPEEK 1.6 membrane and the SPEEK/Y-zeolite/TPA composite membranes for 2.5M initial concentration in the reservoir compartment.	87
Figure 4-22: Methanol crossover flux for the pure SPEEK 1.6 membrane and the SPEEK/Y-zeolite/TPA composite membranes for 2.5M initial methanol concentration in the reservoir compartment.	88

ABSTRACT

NAME OF STUDENT **Mukhtar Bello**

TITLE OF STUDY **Methanol Permeation through Proton Exchange
Membranes of Direct Methanol Fuel Cells**

MAJOR FIELD **Chemical Engineering**

DATE OF DEGREE **May 2006**

Methanol permeation through proton exchange membranes is one of the major constraints inhibiting large scale commercialization of direct methanol fuel cell (DMFC). In the development of membranes for DMFC, it is important to have accurate, reliable, and convenient techniques for determining the methanol permeation rate through the membranes. Five techniques used for measuring methanol permeation through the proton exchange membranes of direct methanol fuel cells have been screened. Electrochemical techniques were found to be more accurate and reliable. Among the electrochemical techniques, potentiometric technique has additional advantages of easier reproducibility of results, convenience, and gives more data points. Thus, potentiometric technique was used to determine methanol crossover flux and permeability of prepared SPEEK/TPA/MCM-41 and SPEEK/TPA/Y-zeolite composite membranes.

SPEEK/TPA/MCM-41 composite membranes with inorganic loadings (TPA/MCM-41) of 10wt % - 30wt % have permeability values of $0.57 \times 10^{-8} \text{ cm}^2 \text{ s}^{-1}$ – $3.51 \times 10^{-8} \text{ cm}^2 \text{ s}^{-1}$. While SPEEK/TPA/Y-zeolite composite membranes with inorganic loadings (TPA/Y-zeolite) of 10wt % -30 wt % have permeability values of $1.71 \times 10^{-8} \text{ cm}^2 \text{ s}^{-1}$ – $4.29 \times 10^{-8} \text{ cm}^2 \text{ s}^{-1}$. These values are low compared to that of pure SPEEK 1.6 membranes; $4.41 \times 10^{-8} \text{ cm}^2 \text{ s}^{-1}$. But when 40wt % of TPA/Y-zeolite loading was used higher permeability value of $7.04 \times 10^{-8} \text{ cm}^2 \text{ s}^{-1}$ was obtained. Better reduction in methanol permeation was observed with lower loadings of the inorganic material (TPA/MCM-41 or Y-zeolite) than with higher loadings. These composite membranes have good potential for use in the direct methanol fuel cell (DMFC) due to their low methanol permeability.

Master of Science
King Fahd University of Petroleum & Minerals
Dhahran, Saudi Arabia
May 2006

ملخص الرسالة

الاسم: مختار بلو.

عنوان الرسالة: نفاذية الميثانول خلال أغشية التبادل البروتوني لخلايا وقود الميثانول المباشر.

التخصص: الهندسة الكيميائية.

تاريخ التخرج: مايو / 2006

تعد نفاذية الميثانول خلال أغشية التبادل البروتوني من العوائق الرئيسية لاستعمال خلايا وقود الميثانول المباشر بشكل تجاري. لتطوير أغشية لخلايا وقود الميثانول المباشر يجب إيجاد تقنيات دقيقة ومريحة ويعتمد عليها لتحديد معدل نفاذية الميثانول خلال هذه الأغشية. تم فحص خمس تقنيات تستعمل لقياس نفاذية الميثانول خلال أغشية التبادل البروتوني لخلايا وقود الميثانول المباشر. وجد ان التقنيات الإلكترونية كيميائية أكثر دقة ويعتمد عليها بشكل أكبر. من بين التقنيات الإلكترونية كيميائية المفحوصة حازت تقنية مقياس فرق الجهد على إجابيات إضافية وهي سهولة إعادة الحصول على النتائج وملاءمتها وأنها تعطي نقاط معلومات أكثر. لذلك تم استعمال تقنية مقياس فرق الجهد لتحديد تدفق ونفاذية الميثانول خلال نوعين من الأغشية المركبة تم تحضيرهما وهما SPEEK/TPA/MCM-41 و SPEEK/TPA/Y-zeolite.

أغشية SPEEK/TPA/MCM-41 المركبة مع حشوات غير عضوية (TPA/MCM-41) بنسب وزنية تتراوح بين 10% - 30% أعطت قيما للنفاذية تتراوح بين 0.57×10^{-8} سم² ث⁻¹ - 3.51×10^{-8} سم² ث⁻¹. بينما أغشية SPEEK/TPA/Y-zeolite المركبة مع حشوات غير عضوية (TPA/Y-zeolite) بنسب وزنية تتراوح بين 10% - 30% أعطت قيما للنفاذية تتراوح بين 1.71×10^{-8} سم² ث⁻¹ - 4.29×10^{-8} سم² ث⁻¹. هذه القيم تعتبر صغيرة مقارنة بها لأغشية SPEEK 1.6 النقية؛ 4.41×10^{-8} سم² ث⁻¹. لكن عند استعمال حشوة TPA/Y-zeolite بنسبة وزنية 40% تم الحصول على قيمة أكبر للنفاذية ومقدارها 7.04×10^{-8} سم² ث⁻¹. تم ملاحظة تحسن في انفاص قيمة نفاذية الميثانول عند استعمال حشوات غير عضوية (TPA/MCM-4 or Y-zeolite) بنسب قليلة أفضل منه عند استخدام نسب عالية. هذه الأغشية المركبة تمتلك إمكانية جيدة لاستعمالها في خلايا وقود الميثانول المباشر نظرا لقيمتها القليلة لنفاذية الميثانول.

CHAPTER 1

1 INTRODUCTION

The search for efficient and cleaner energy conversion technology and the need for alternative renewable fuels have increased the investments on fuel cell research and technology in the last years. Fuel cells are very promising energy conversion devices with numerous possible applications. They have high energy efficiency, low or zero emissions, simplicity, and flexibility in power supply. These properties make them attractive when compared with the existing, conventional energy conversion technologies. Fuel cells can generate power from a fraction of watt to hundreds of kilowatts. Because of this, they may be used in almost every application where local electricity generation is needed. Applications such as automobiles, utility vehicles, scooters, bicycles, and submarines have been already demonstrated [1].

A fuel cell is an electrochemical engine which continuously converts the chemical energy of a fuel into direct current electrical energy. This is analogous to the combustion process which occurs in a heat engine, but in a fuel cell this can take place at much lower temperature, high energy efficiency and reduced polluting emissions. For these reasons, fuel cells are expected to play an important role in the replacement of the internal combustion engine. A fuel cell is in some aspects similar to a battery. It has an

electrolyte, and negative and positive electrodes, and it generates direct current electricity through electrochemical reactions. However, unlike a battery, a fuel cell supplies power as long as there is a supply of fuel and oxidant. Also, the electrodes in a fuel cell do not undergo chemical changes. Research has been conducted and is currently being conducted into several types of fuel cells.

Hydrogen as an energy carrier is the common fuel for fuel cells but is not readily available. Presently organic fuels are steam reformed to hydrogen-rich gas before entry into the anode side of a fuel cell. The size of the system due to the presence of the reformer complicates the design. In addition, because the concept of “Hydrogen Energy Economy” is yet to be fully realized there are no infrastructural networks to support the distribution of hydrogen easily. Thus, research efforts are geared towards designing a fuel cell that would directly oxidize a liquid fuel at the anode and will have improved overall cell performance. Direct methanol fuel cell (DMFC), where methanol fuel is supplied directly to the anode of the cell is one of the promising candidates. Much attention is now focused on it especially in Europe and the United States. DMFC technology is attractive for the automobile industry and is being seen as a future energy source for mobile power applications. It has the advantage of not requiring a fuel reformer, allowing simple and compact designs. Also, infrastructure built for gasoline can be used without significant alteration and changes in power demand can be accommodated simply by alteration in supply of methanol feed. Due to low operating temperature of the cell there is no production of NO_x [2]. Methanol is stable in contact with acidic membranes, has limited toxicity, and high energy density (3800 kcal/liter) compared to hydrogen at 360atm (658

kcal/liter). It is cheaper to manufacture, and is easier to handle and transport (liquid at room temperature) [3].

However, despite these advantages, there are two major constraints inhibiting large scale commercialization of a DMFC. Problems relating to Nafion[®] membranes which are used as polymer electrolyte membranes and low activity of the methanol electro-oxidation catalysts. Nafion[®] membranes permits methanol crossover from the anode to the cathode and is costly. Its proton conductivity decreases at high temperature ~ above 90 °C. Operating the fuel cell in the temperature range up to around 150 °C would improve the reaction kinetics and reduce the catalyst poisoning by CO, but dehydration leads to a drastic reduction of the Nafion[®] performance above 100 °C. In both PEMFCs and DMFCs, polymer electrolyte membranes are used, which have proton-conducting pathways produced by fixed functional groups or proton conducting gel. Nafion[®], a perfluorosulfonate membrane developed by DuPont dominates the market of polymer electrolyte membranes for fuel cell owing to high ionic conductivity in its hydrated state and good thermal and chemical stability. While it has shown very good performance in the PEMFCs, in the DMFCs it does not meet the requirements for sufficiently low methanol permeability. It has been reported that over 40% of the methanol can be wasted in DMFCs across such membranes [4]. This crossover is caused by diffusion of methanol due to concentration gradient and by molecular transport due to electro-osmotic drag.

The methanol transported through the membrane reduces the effective area of the cathode by utilizing cathode Pt sites for the direct reaction between the methanol and oxygen.

This leads to secondary reactions, mixed potentials, decreasing energy and power density, generation of additional water that must be managed, increasing oxygen stoichiometric ratio, and hence reduced overall performance [5]. Thus, the DMFC technology would greatly benefit both in terms of energy efficiency and output voltage from a drastic reduction of the methanol crossover which would contribute to its successful commercialization. However, recent studies have shown that even a 20% efficient cell far exceeds the advanced lithium batteries performance thus, making the DMFC an attractive option for portable power supply. But still efforts are being made in order to develop membranes with low methanol diffusivity, without compromising on other qualities such as; high ionic conductivity, good chemical and thermal stability, and cost. This includes modification of the Nafion[®] membranes, development of polymer/inorganic mineral acid composite membranes, partially fluorinated polymers, non fluorinated polymers and their combinations, and so forth. In recent works, it has been shown that sulfonated poly (ether ether ketone) (SPEEK) is very promising for fuel cell application as it possesses low methanol permeability, good thermal stability, mechanical strength and moderate conductivity. SPEEK/HPAs/Y-zeolite and SPEEK/ HPAs /MCM-41 composite membranes with high proton conductivity and good thermal stability were prepared but their methanol permeability has not been studied [6].

A number of techniques both electrochemical and non-electrochemical have been developed to measure the methanol permeability of polymer membranes using either a simulated fuel cell (diffusion cell set-up) or a real fuel cell. The non-electrochemical techniques either rely on measuring the concentration of CO₂ that is produced by

oxidation of methanol at the cathode or the concentration of the diffused methanol by gas chromatography, IR sensor, mass spectrometry etc, to find the methanol flux across the membrane. While in electrochemical techniques a parameter is measured like current density, potential at open circuit voltage, limiting current density etc, which is related to the methanol concentration. In the development of membranes for DMFC, it is important to have accurate, reliable, and convenient techniques of measuring the membranes methanol permeability. In this work, five techniques including both electrochemical and non electrochemical were screened in order to suggest the best one for measuring the membranes methanol permeability. Potentiometric technique has been found to be the best. It was used in determining the methanol permeability of the prepared SPEEK/TPA/Y-zeolite and SPEEK/TPA/MCM-41 composite membranes.

1.1 Objectives

The objectives of this research work are:

- 1) To determine best measurement technique(s) for methanol permeation through proton exchange membranes.
- 2) To use the best technique to determine methanol permeability of SPEEK/TPA-/MCM-41 and SPEEK/TPA/Y-zeolite composite membranes.

CHAPTER 2

2 LITERATURE REVIEW

2.1 Fuel Cells

Fuel cells have excited the minds of theoretical scientists and practical technologists for over 100 years, ever since the first experiments of W. R. Grove showed that the electrolysis of water was a reversible process, and W. Oswald provided the basic thermodynamic equations showing the definite advantages of “Low Temperature Electrochemical Oxidation” over “High Temperature Combustions” of fuels [7]. Fuel cells produce electricity continuously through the electrochemical oxidation of a fuel. Recent years have seen an upsurge in interest in fuel cells for a range of applications, in particular for transport and small scale static power systems. Depending on the load, fuel, cell type and conditions of operation a single cell has a potential of 0.5V to 1.0 V. To yield a sufficient high voltage, the cells are stacked, or electrically connected in series.

2.1.1 Types of Fuel Cells

Fuel cell systems can be classified according to the working temperature: High, medium and low (ambient) temperature systems or referring to the pressure of operation: high,

medium and low (atmospheric) pressure systems. They may be further distinguished by the fuels and/or the oxidants they use. For practical reasons fuel cell systems are simply distinguished by the type of electrolyte used. The following names and abbreviations are now frequently used in publications: Alkaline fuel cells (AFC), proton exchange membrane fuel cells (PEMFC), direct methanol fuel cells (DMFC), phosphoric acid fuel cells (PAFC), molten carbonate fuel cells (MCFC), and solid oxide fuel cells (SOFC). Table1 shows the classification.

Table 2-1: Types of Fuel Cells

Fuel Cell System	Temperature Range (°C)	Efficiency (%)	Electrolyte	Application Area
AFC	60-90	50-60	KOH	Space Application
PEMFC	50-80	50-60	Polymer membranes	Automobile
DMFC	50-150	50-55	Polymer membranes	Automobile/Portable Power generation
PAFC	160-220	55-60	Phosphoric acid	Stationary Power generation
MCFC	620-660	60-65	$\text{Li}_2\text{CO}_3/\text{Na}_2\text{CO}_3$	Stationary Power generation
SOFC	800-1000	55-65	$\text{ZrO}_2/\text{Y}_2\text{O}_3$	Stationary Power generation

2.1.2 Direct Methanol Fuel Cells (DMFC)

Whilst the power efficiencies of common H_2/O_2 fuel cells continue to show steady improvements, there remain problems with the use of hydrogen as the active fuel: either this hydrogen must be obtained by in situ reformation of solid or liquid C-H fuels, such as petroleum, coal or methanol, or it must be pre-purified and stored as the gas under pressure, or in the form of an admixture with a metal alloy, carbon or some other absorbents [8]. In all of these cases, either there is a considerable weight penalty or there is increased engineering complexity, adding to costs. It remains highly desirable to design a fuel cell that would directly oxidize a liquid fuel at the anode, but retain the high power/weight ratio of the solid-polymer electrolyte fuel cells. One such fuel cells now under active development in Europe and the USA, is the direct methanol fuel cell. Methanol possesses a number of advantages as a fuel: it is a liquid up to around 65°C , and therefore easily transported and stored and dispensed within the current fuel network; it is cheap and plentiful, in principle renewable from wood alcohol, and the only products of combustion are CO_2 and H_2O . The advantages of a direct methanol fuel cell are: changes in power demand can be accommodated simply by alteration in supply of the methanol feed; the fuel cell operates at temperatures below $\sim 150^\circ\text{C}$ so there is no production of NO_x , methanol is stable in contact with mineral acids or acidic membranes, and it is easy to manufacture; above all, the use of methanol directly as an electrochemically active fuel hugely simplifies the engineering problems at the front end of the cell, driving down complexity and cost. Figure 2-1 shows a schematic of a DMFC.

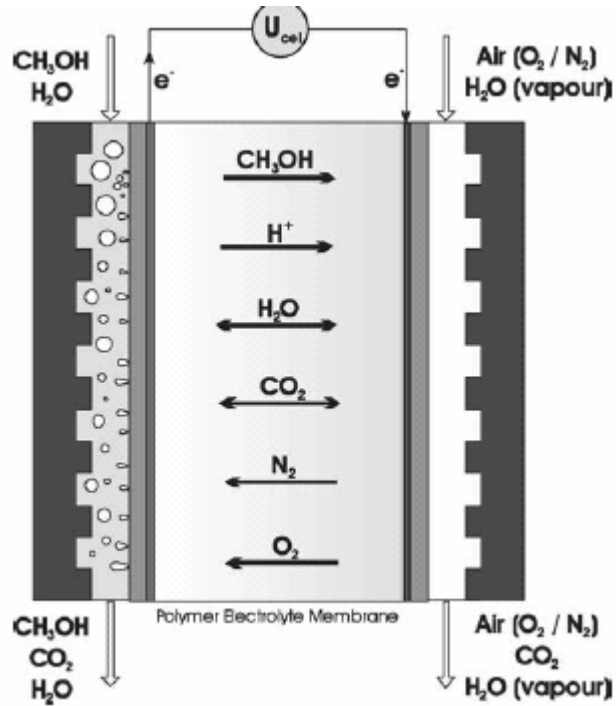
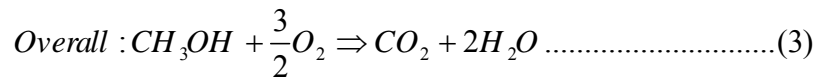
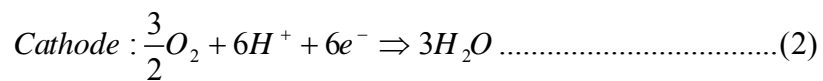
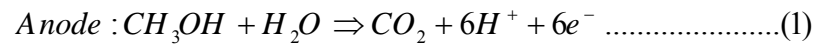


Figure 2-1: Schematic diagram of a DMFC



The basic problems currently faced by the direct methanol fuel cell are [9]:

- * The anode reaction has poor electrode kinetics, particularly at lower temperatures, making it highly desirable to identify improved catalysts and to work at as high a temperature as possible.
- * The cathode reaction, the reduction of oxygen, is also slow: the problems are particularly serious with aqueous mineral acids, but perhaps not so serious with acidic polymer membranes. Nevertheless, the overall power density of the direct methanol fuel cells is much lower than the $600+ \text{ mW cm}^{-2}$ envisaged for the hydrogen fuelled solid polymer electrolyte fuel cell (SPEFC).
- * Perhaps of greatest concern at the moment is the stability and permeability of the current perfluorosulfonic acid membranes to methanol, allowing considerable fuel crossover, and, at the higher temperatures needed to overcome limitations in the anode kinetics, degradation of the membrane both thermally and through attack by methanol itself.
- * The fact that methanol can permeate to the cathode leads to poor fuel utilization, the appearance of a mixed potential at the cathode, since conventional cathode catalysts are based on platinum, which is highly active for methanol oxidation at the higher potentials encountered at the cathode. Experimentally, this problem has been tackled both by seeking alternative oxygen reduction catalysts and by increasing the Pt loading substantially; the latter clearly increases costs significantly.

In spite of these difficulties, the DMFCs have the capability of being very cheap and potentially very competitive with the internal combustion engine, particularly in niche city driving applications, where the low pollution and relatively high efficiency at low

load are attractive features. Performances from modern single cells are highly encouraging especially with the tremendous efforts being made to provide methanol impermeable proton exchange membranes. Proton exchange membranes (PEMs), have assumed great importance especially due to their applications in fuel cells. However, the dominantly used per fluorinated membrane; Nafion[®], displays adequate proton conductivity when hydrated but suffers some disadvantages, such as; methanol permeation, high cost and poor hydrophilicity at high temperatures ~ above 90 °C [10]. These drawbacks have prompted research into modifying the Nafion[®] membranes and developing alternative membranes based on partially per fluorinated ionomers and hydrocarbon polymers.

2.2 Nafion[®] membranes Modification

Nafion is a non-cross-linked ion-exchange polymer comprising of a per fluorinated backbone with sulfonate ionic groups attached to pendant side chains. Because of its structure, phase separation occurs in hydrated state between the hydrophilic regions and the hydrophobic ones and ionic clusters are formed. This morphology with discrete hydrophobic and hydrophilic regions gives the material very good properties. The well connected hydrophilic domain is responsible for its excellent ability to allow transport of protons and water easily while the hydrophobic domain provides the polymer with the morphological stability and prevents the polymer from dissolving in water. This explains the exceptional transport efficiency in hydrated Nafion. Figure 2-2 illustrates the chemical structure of Nafion.

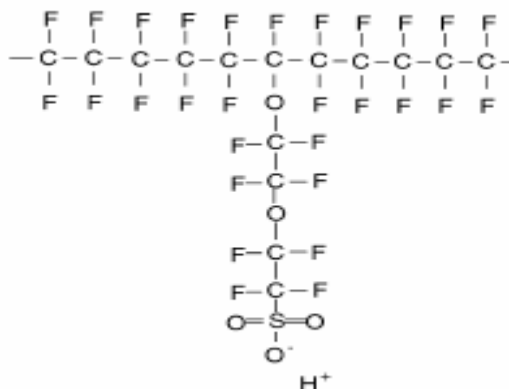


Figure2-2: Chemical Structure of Nafion.

Water is necessary for the transport of protons but it also has high affinity to methanol transport. One way of reducing methanol permeation is to modify the Nafion[®] membranes by blending with either organic or inorganic materials.

2.2.1 Nafion/Organic Blend Membranes

Nafion/polypyrrole [12-13]. Nafion/poly (1-vinylimidazole) [14], Nafion/poly furfuryl alcohol (PFA) [15], Nafion/poly vinylidene fluoride (PVdF) [16], and Nafion/polyvinyl alcohol (PVA) [17] composite membranes, have low methanol permeability compared to the plain Nafion membranes and their proton conductivity is comparable with that of Nafion[®] membranes. However, choice of appropriate quantity of the methanol barrier material and thickness of the composite membranes is important in achieving the desired methanol permeation reduction.

Also, membranes based on the aromatic poly (ether ether ketone) (PEEK) have shown high potentials for DMFC applications due to their low methanol permeability, good

thermal stability and mechanical properties and the proton conductivity can be controlled by the degree of sulfonation. Many studies have indicated that SPEEK membranes have the ability to reduce the problems associated with high methanol crossover in DMFCs. Multilayered membranes containing a thin inner layer of SPEEK as a barrier and two outer layers of recast Nafion, fabricated by hot-pressing significantly reduced methanol permeation in DMFC [18]. However, appropriate sulfonation degree and thickness of the inner SPEEK layer is particularly important in achieving the desired Nafion-SPEEK-Nafion composite membranes. Also, Nafion-SPEEK-Nafion composite membrane prepared by immersing the SPEEK in Nafion-containing casting solution has low methanol permeability and a lesser ionic conductivity compared to that of pure Nafion[®] membranes [19].

2.2.2 Nafion/Inorganic Blend Membranes

Addition of silica to Nafion enhances water retention in the membrane and enables the operation of the fuel cell above 130°C. A similar method for retaining water in Nafion[®] at higher temperatures by incorporating silica and titanium dioxide into a Nafion[®] composite to enable its use in DMFC has also been reported [20]. Though the membrane could achieve a significant improvement in proton conductivity it may not retard methanol permeation. But elsewhere, it has been indicated that Nafion/silica hybrid can decrease the methanol crossover if appropriate silica content is used [21-22]. Nafion membranes containing additives such as silicon dioxide particles (Aerosil[®]) and molybdophosphoric acid will have higher proton conductivity but the combined parameter of methanol permeability and proton conductivity is less than that of

commercial Nafion[®] membrane [23]. This is likely due to a structural modification of the membrane because of the addition of inorganic components and having new interfacial polymer-particle particles.

Also, deposition of clay-nanocomposite thin films on the Nafion membranes by layer-by-layer assembly could enhance resistance of the membrane against methanol crossover [24]. Multilayer of clay nanoparticles and ionic polyacetylene PEPy-C18 deposited on Nafion[®] membranes to produce appropriate bilayer nanocomposite films with a suitable thickness could reduce methanol permeation of the Nafion[®] membrane significantly without much negative effect on its proton conductivity.

Another means of modifying Nafion[®] membranes attracting interest is that of impregnation of Pd on the Nafion[®] membranes. The Nafion[®] membranes modified by impregnating Pd- nanophases allow selective transport of smaller water molecules or hydrogen ions, while the passage of larger molecules would be restricted [25]. A well dispersed Pd nanophase in the Nafion is effective in preventing or reducing methanol crossover through the membrane while at the same time maintaining good proton conductivity. Several other studies [26-30] using different deposition or coating techniques show that Nafion/ Pd composites can significantly reduce methanol permeation compared to bare Nafion and does not change the membrane conductivity resulting into better cell performance. This could be due to the fact that during the deposition of Pd, the -SO₃H group is not affected but the presence of the Pd reduces the methanol permeation.

Many other inorganic materials when blended with Nafion[®] membranes are likely to show improvement on the membranes properties such as thermal stability, proton conductivity and lower methanol permeation. Calcium phosphate/Nafion composite membranes [31], Nafion doped with cesium cations [32], etc have shown evidence of good performance in the operation of DMFCs. The presence of cesium ions in the membrane, specifically in the water-rich domains, will cause a remarkable reduction of methanol permeation. However, the proton conductivity could be depressed to a lesser extent by the presence of the cesium ions in the membrane. But, at ambient conditions, the combined parameter of both proton conductivity and methanol permeability shows better performance of Cs⁺-doped membranes than the Nafion[®] 117 membranes in the operation of DMFC.

2.3 Alternative Membranes

2.3.1 Sulfonated Poly Ether Ether Ketone (SPEEK) Membranes

Membranes based on the aromatic poly (ether ether ketone) (PEEK) seem very promising because in addition to their low methanol permeability they possess good mechanical properties, thermal stability and the proton conductivity can be controlled through the degree of sulfonation. The main difference between the Nafion[®] membranes and SPEEK membranes which makes the latter less permeable to methanol can be attributed to the difference in their microstructure. As shown in Figure 2-3, in SPEEK membranes there is less pronounced hydrophilic/hydrophobic separation as compared to Nafion[®] membrane and the flexibility of the polymer backbone of SPEEK produce narrow proton channels

and a highly branched structure, which baffle the transfer of methanol. Thus, SPEEK membranes have lower electro osmotic drag and methanol permeability.

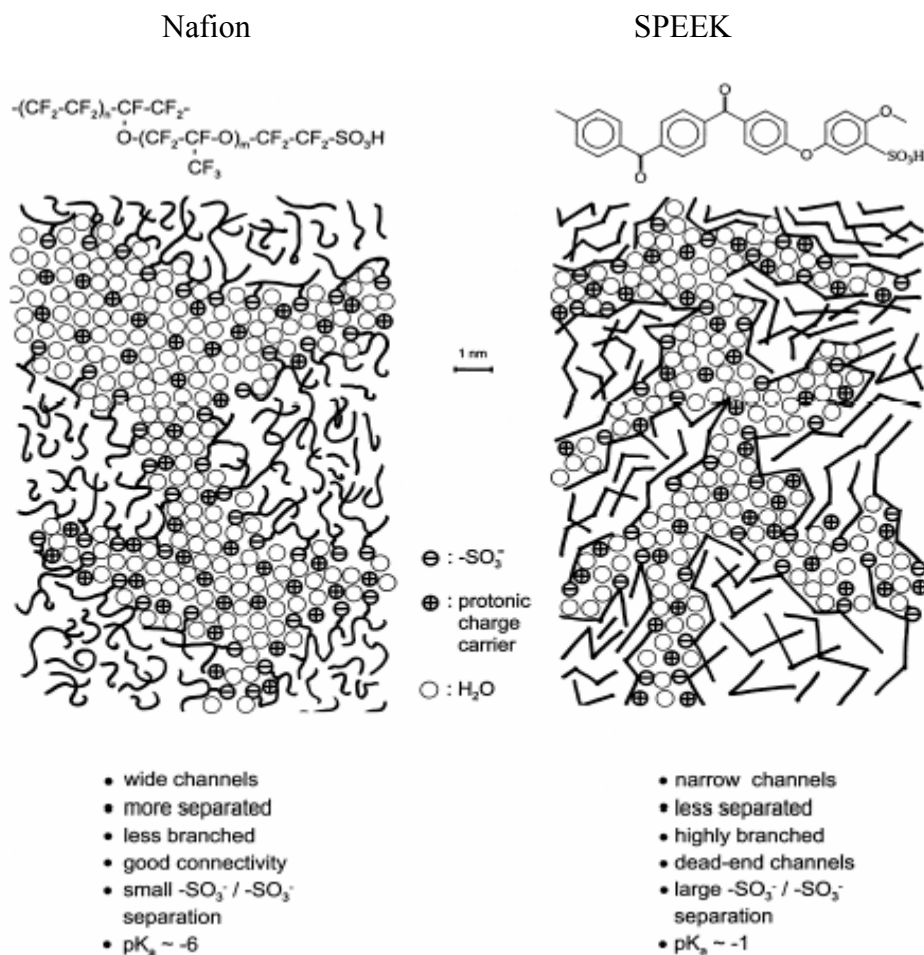


Figure 2-3: Schematic representation of the microstructure of Nafion and SPEEK.

Proton conductivity of the SPEEK membranes with degree of sulfonation of 39 % and 47 % is close to that of Nafion[®] 115 membranes while the methanol permeability is an order lower than that of Nafion[®] 115 membranes under the same condition [34]. At 80 °C, the overall DMFC performance of the SPEEK membranes is better than that of

Nafion[®] 115 membrane. Furthermore, SPEEK membranes with methanol diffusion coefficient values of $5 \times 10^{-8} \text{ cm}^2/\text{s}$ to $3 \times 10^{-7} \text{ cm}^2/\text{s}$ at 25 °C which is lower compared to that of Nafion[®] membranes (10^{-6} to $10^{-5} \text{ cm}^2/\text{s}$) have been synthesized [35].

Sulfonated poly (ether ether ketone ketones) SPEEKKs and sulfonated poly (ether ketone ketone) SPEKK membranes have been synthesized. They allow lower methanol permeation than the Nafion[®] membranes under the same condition [36-37]. The SPEEKKs membranes show high thermal stability, good proton conductivities and methanol diffusion coefficients of 6.6×10^{-7} to $8.6 \times 10^{-7} \text{ cm}^2/\text{s}$. However, the SPEEKKs membranes did not show better performance over SPEEK membranes in the DMFC application.

2.3.2 SPEEK Composite Membranes

Although methanol permeability values of SPEEK membranes are low compared to that of Nafion[®] membranes, their proton conductivity is not as good as that of Nafion[®] membranes. In order to improve the proton conductivity, various inorganic materials such as SiO₂, ZrO₂, heteropolyacids and phosphates has been successfully used to enhance proton conductivity, and control the methanol permeability as can be seen in Figure 2-4 [38-39].

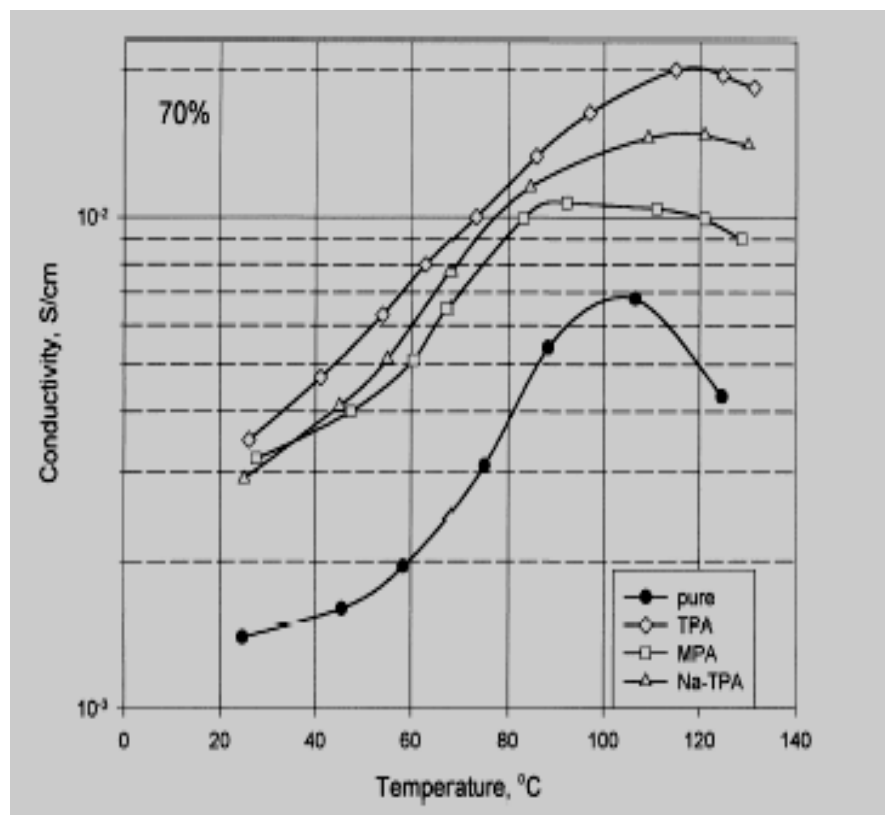


Figure 2-4: Effects of different HPAs on the conductivity of composite membranes as a function of temperature (70% DS).

However, the incorporation of heteropolyacids alone into the matrix of SPEEK could lead to an increase in water and methanol permeation through the membrane which is highly undesirable for application in the DMFC [40]. The permeability can be remarkably reduced by adding appropriate amount of zirconium oxide (ZrO_2). The inorganic network reduces the methanol and water crossover through the membrane and also decreases the bleeding out of the heteropolyacids.

Composite membranes prepared by incorporating Laponite and Montmorillonite (MMT) into a partially sulfonated PEEK polymer also help to reduce swelling in hot water significantly and reduce methanol permeability without a serious reduction in the proton conductivity [41]. The membranes are thermally stable up to 240 °C and have good conductivity. Figure 2-5, shows that the methanol flux across SPEEK/Lapo10 composite membrane is far lower than that of Nafion[®] 115 membrane. The SPEEK membrane also displays lower methanol permeability compared to the Nafion[®] 115 due to the difference in their microstructure.

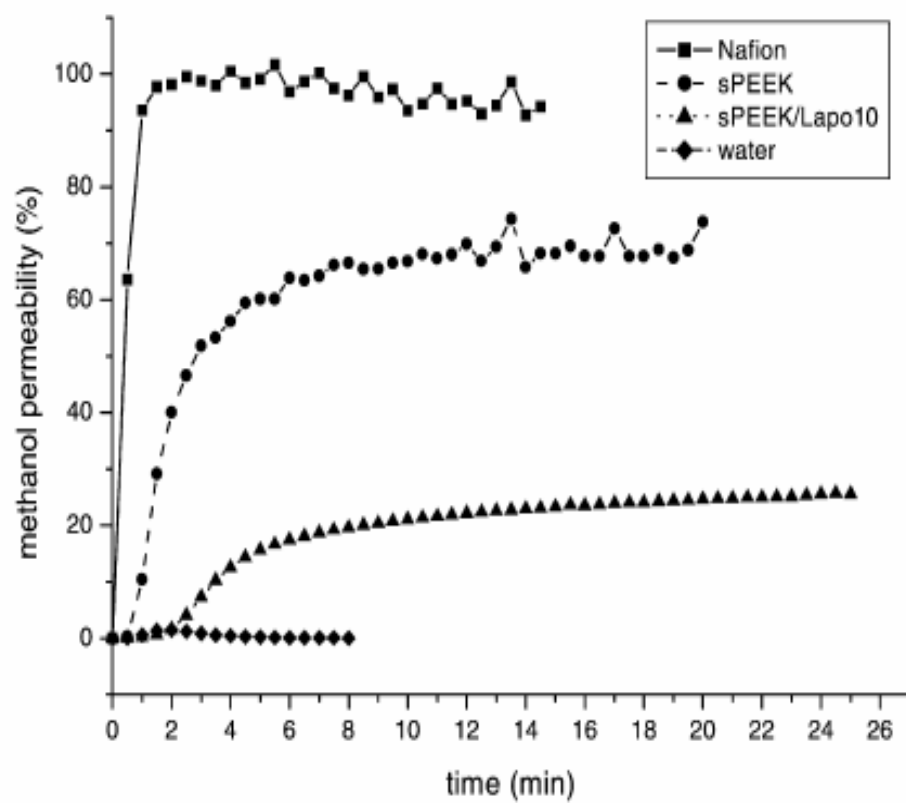


Figure 2-5: Methanol permeability in Nafion® 115 and composite membranes.

Composite membranes prepared by incorporating BPO_4 fine powder into partially sulfonated PEEK polymer have conductivity higher than that of pure SPEEK and in some cases the conductivity can exceed that of HPAs/SPEEK composite membranes. The composite membranes are mechanically strong and flexible at $\text{DS} < 80\%$ and their conductivity is not affected by storage in water for several months. These membranes ($\text{BPO}_4/\text{SPEEK}$) offer less expensive alternative, and thus, have great potential for use in DMFC.

Also, SPEEK composite membranes prepared by blending different proportions of solid proton conductors; TPA and MPA loaded Y-zeolite into the SPEEK polymer matrix have shown promise of good performance. The conductivity of the composite membranes increases as the loading of solid inorganic material increases from 10 wt. % to 40 wt. % and also with temperature [6]. The maximum conductivity of SPEEK/TPA/Y-zeolite is in the order of 10^{-2} S/cm and the membranes are stable up to 140°C . However, methanol permeability study of these composite membranes is one of the objectives of this research.

2.3.3 Sulfonated Poly-Styrene Membranes (SPS)

Commercial non-cross-linked poly (styrene) can be partially sulfonated to various degrees, obtaining a homogeneous distribution of the sulfonic acid groups in the polymer. Membrane cast from these materials exhibit proton conductivity similar to that of Nafion[®] membrane [42]. In the same way, the permeability to methanol also increases

with the density of the sulfonate groups in the polymer. However, even at the highest degree of sulfonation, the permeability of SPS is comparatively small.

2.3.4 SPS/PTFE Composite Membranes

Sulfonated polystyrene/polytetrafluoroethylene (SPS/PTFE) composite membranes prepared for DMFC application show comparable ion conductivity and lower methanol permeability than Nafion[®] 117 membrane, indicating that the composite membranes can compete well with the Nafion[®] membranes in the DMFC application [43]. The sulfonated composite membranes have higher water content than the Nafion[®] membrane, presumably due to the higher sulfonic acid content with its strong affinity to water, which would be expected from the higher ion-exchange capacity (IEC) values. The water content of the composite membranes has an inverse relationship with the PTFE content because more cross linked networks reduce the membrane free volume and the swelling ability. This shows that the water content, which greatly influences the methanol permeation and ion conductivity, can be controlled by changing the ratio of monomer (styrene) to cross linker TFE.

However, as the PTFE content is increased, the methanol diffusivity decreases but ion conductivity also decreases fairly. A membrane with highest value of the ratio of ion conductivity to the methanol permeability (Φ = ion conductivity/methanol permeability) is regarded as the best. It is evident from Figure 2-6, that ion conductivity to methanol permeability ratio (Φ) is higher in the SPS/PTFE composite membranes than in Nafion[®] membranes.

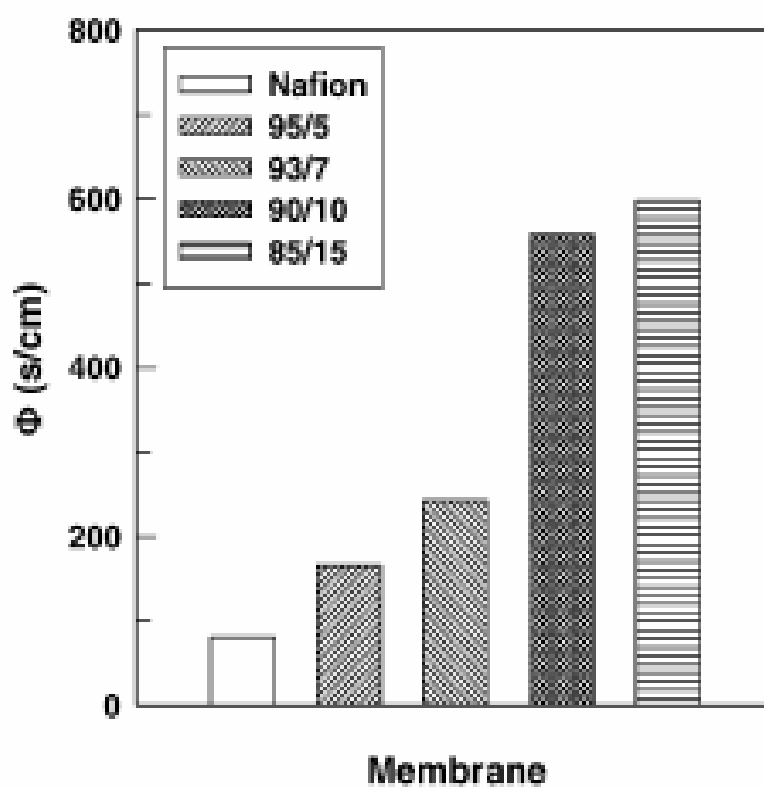


Figure 2-6: Comparison of the Φ (S/cm) parameter of Nafion and the SPS/PTFE composite membranes.

2.3.5 Poly (Vinylidene) Fluoride (PVdF) Composite Membranes

Composite poly (vinylidene) fluoride (PVdF)-based proton conducting membranes have low methanol permeation, high proton conductivity (which shows less dependence on the water content), and low cost, [44]. Polymer blends of 1:9 ratios PVdF/SPEEK have methanol permeability of about 5% that of Nafion[®] 115 under the same testing condition. However, the proton conductivity of this composite membrane is 1.75×10^{-3} S/cm, which is lower than that of Nafion[®] 115 membrane. Furthermore, PVdF/poly styrene sulfonic acid (PSSA) composite membranes also have low methanol crossover during operation of DMFCs compared to the Nafion[®] membranes [45, 46]. The low methanol permeation, good proton conductivity, stability and excellent water management of PVdF/PSSA membranes improve fuel cell performance. Poly styrene sulfonic acid (PSSA) is also a good blending material for proton exchange membranes. PSSA/polyvinyl alcohol has low methanol permeability and good proton conductivity, which can enable them to perform well in the DMFC operation.

2.3.6 Poly-Ethylene Tetrafluoroethylene -based Membranes

Methanol permeation through poly (ethylene tetrafluoroethylene) (ETFE) membrane investigated at temperatures of 30 °C, 50 °C and, 70 °C showed 90% reduction in the permeability values compared to the Nafion[®] 115 membrane [47]. In addition, the ETFE-based membranes are cheaper, have good chemical and mechanical stability. However, the efficiency of this membrane is about 40-60% lower than the efficiency of the DMFCs with the Nafion[®] 115 membrane due to lower proton conductivity and high IR-losses of

the MEAs. But radiation grafted polymer electrolyte membranes prepared using ETFE, poly vinylidene fluoride (PVdF) and low-density polyethylene (LDPE) as base polymer films and polystyrene sulfonic acid (PSSA) as proton-conducting groups have good performance in the DMFCs [48]. With appropriate degree of grafting and membrane thickness, membranes with suitable conductivity and low methanol permeation superior to Nafion[®] membranes can be produced.

2.3.7 Polyphosphazene-based Membranes

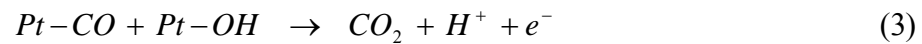
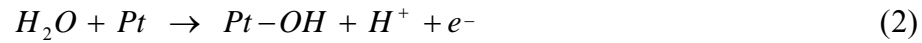
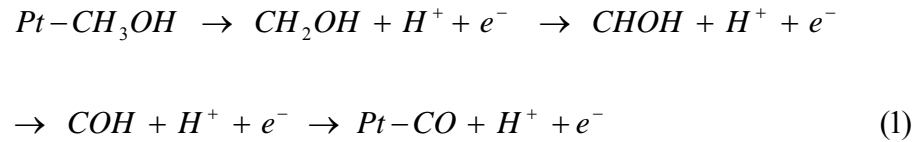
Studies of methanol crossover in proton-conducting polyphosphazene membranes show that polyphosphazene-based proton-exchange membranes have low methanol permeability and good proton conductivity [49, 50]. These membranes have been tested in the DMFCs and have shown good performance.

2.3.8 Polyvinyl alcohol/mordenite

Polyvinyl alcohol/mordenite composite membrane prepared using appropriate quantity of mordenite and heat treatment could significantly reduce the permeation of methanol molecules [51]. However, to achieve this improvement, there should be a suitable tailoring of the transport properties between the polymer and the zeolite phases. The zeolite phases allow the transport of electrons but inhibit that of methanol molecules, thus, making the membrane less permeable to methanol.

2.4 Improved Electro oxidation Catalysts

Some attempts have been made to improve the activity of the electro oxidation catalyst which is also seen as helping to reduce the methanol permeation. When the catalyst activity is very high more of the methanol is expected to get oxidized instantly there by reducing the amount permeating to the cathode side. Pt – based electro oxidation catalysts display the necessary stability in the acidic environment of DMFC, although much progress is still needed, they show significant activity. Reaction mechanism for methanol oxidation in aqueous electrolyte has been suggested as follows [52]:



One problem associated with the methanol dehydrogenation on the Pt-electrode surface is poisoning of the electrode by CO formed as an oxidation intermediate. The CO can adsorb very strongly on the Pt surface blocking the active sites and causing a large decrease in the electrode performance. In order to overcome the poisoning problem, Pt-Ru alloy catalysts have been in use. Ru can dissociate water at lower potential to create oxygen-containing surface groups needed to convert CO to CO₂ [53]. It forms Ru-OH_{ads} species at lower potentials, which helps to oxidize the adsorbed CO through the bifunctional mechanism. Weakening of the Pt-CO bond takes place in the alloy, resulting

in a lower CO coverage and an increased mobility similar to what happens with other CO-tolerant Pt alloys, via the modification of the Pt electronic structure by alloying.

So far, the Pt-Ru alloy has shown the most promising performance for the hydrogen oxidation reaction in the presence of CO and also for the oxidation of methanol. Carbon black has been used as support for the metal nano particles, particularly Vulcan XC-72 (Cabot) which has a surface area of 240 m²/g. Methanol oxidation starts at lower potential values for all the Pt-Ru/C catalysts than for Pt/C anodes. Comparison of electrodes prepared with Pt and Pt-Ru as electro catalyst supported on nano tubes and those prepared with the most usual support, Vulcan XC-72 shows multi wall carbon nano tubes produce Pt-Ru/MWNT catalysts with better performance than on other supports, particularly with respect to those prepared with the traditional Vulcan XC-72 carbon powder [54].

2.5 Methanol Crossover Measurement Techniques

It is important to have accurate, reliable, and convenient methods of measuring the methanol permeation in the development of membranes for DMFC. A number of methods have been developed to determine the methanol permeability of membranes using both a real DMFC and simulated system.

2.5.1 Monitoring CO₂ from cathode of DMFC

Early studies on the methanol permeation problem in the DMFC revealed that the methanol permeating to the cathode side oxidizes to CO₂ [55]. Since then a widely used technique to measure the methanol permeation in a DMFC is to determine the CO₂ content of the cathode exhaust gas flux using an optical IR CO₂ sensor [56-58]. However, during the operation of DMFC part of the CO₂ produced in the anodic catalyst layer permeates through the perfluorosulfonate membrane to the cathode side as shown in Figure 2-7. Also, as can be observed, there is incomplete oxidation of the methanol at the cathode. Studies have confirmed this anodic CO₂ contribution and neglecting it could result in overestimation of the methanol flux value [59, 60].

For low methanol concentration, methanol permeation reduces with increasing current density which implies low production of CO₂ at the cathode. Thus, at high current densities and low methanol concentration (<1M) the amount of CO₂ crossing from the anode to the cathode can even be higher than the amount of CO₂ produced at the cathode by methanol oxidation [61]. Therefore, the presence of anodic CO₂ and incomplete oxidation of methanol at the cathode side have to be considered in order to avoid reporting wrong values for the methanol crossover flux. The contribution of CO₂ coming from the feed air at the cathode should also be considered for accurate measurement. Precise amount of anodic CO₂ permeating through the membrane to the cathode side can be obtained using a methanol tolerant cathode layer which does not oxidize the permeated methanol. Also, using gravimetric determination of BaCO₃ the CO₂ produced both at the anode and the cathode can be analyzed [62].

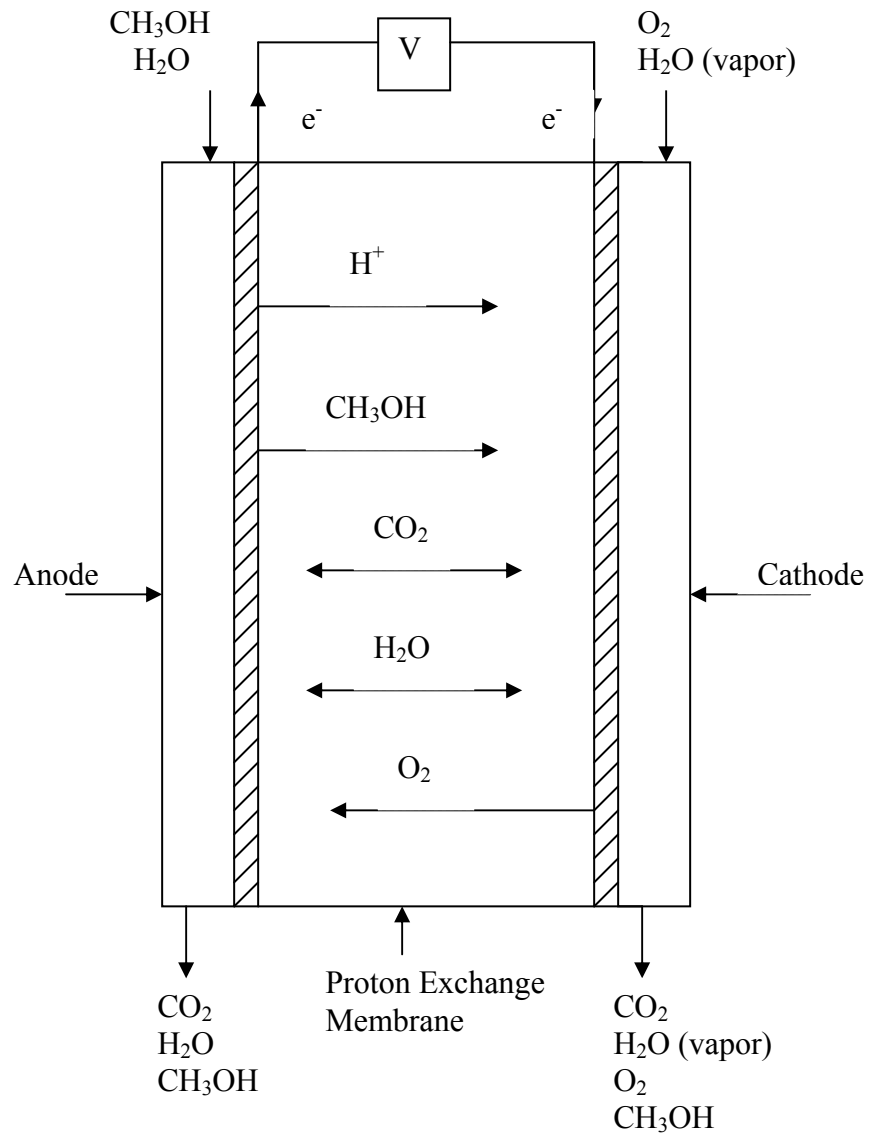
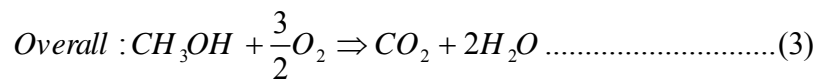
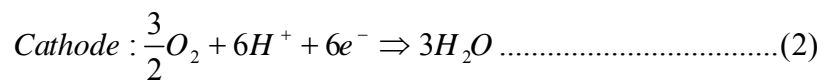
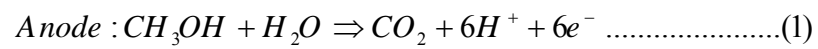


Figure2-7: Schematic diagram of DMFC showing CO_2 crossover



2.5.2 Open Circuit Voltage (OCV)

Open circuit voltage values obtained using a DMFC can be used to determine the membrane diffusivity. Barragan et al [63] studied the effect of varying cathode pressure between 1 atm to 5 atm on the OCV of a DMFC while maintaining the anode pressure at atmospheric condition. They developed a model equation which relates the OCV with the membrane diffusivity and found the diffusivity of Nafion® membranes to be in the order of $10^{-5} \text{ cm}^2/\text{s}$.

$$OCV = E_{cell}^o - D^o \ln \left(\frac{P_2}{P_1} \right) - \frac{\gamma}{M + G (P_2 - P_1)} \quad (1)$$

Where P_1 and P_2 are the anode and cathode pressures respectively,

$$\gamma = \chi \frac{D_{mem} C^*}{\delta_{mem}}$$

$$D^o = \Delta N \frac{RT}{\eta_{cat} F}$$

$$M = \frac{D_{mem} \delta_{el}}{D_{el} \delta_{mem}} + \frac{D_{mem}}{\delta_{mem} k} + 1 \quad \text{And} \quad G = \frac{K_{mem}}{k \delta_{mem}}$$

Figure 2-8 shows the OCV values versus cathode pressure for the Nafion 115 membrane. These OCV values can be fitted to the model equation by using a three-parameter (γ , M and G) non-linear regression method for the membranes. The parameters are function of the membrane diffusivity.

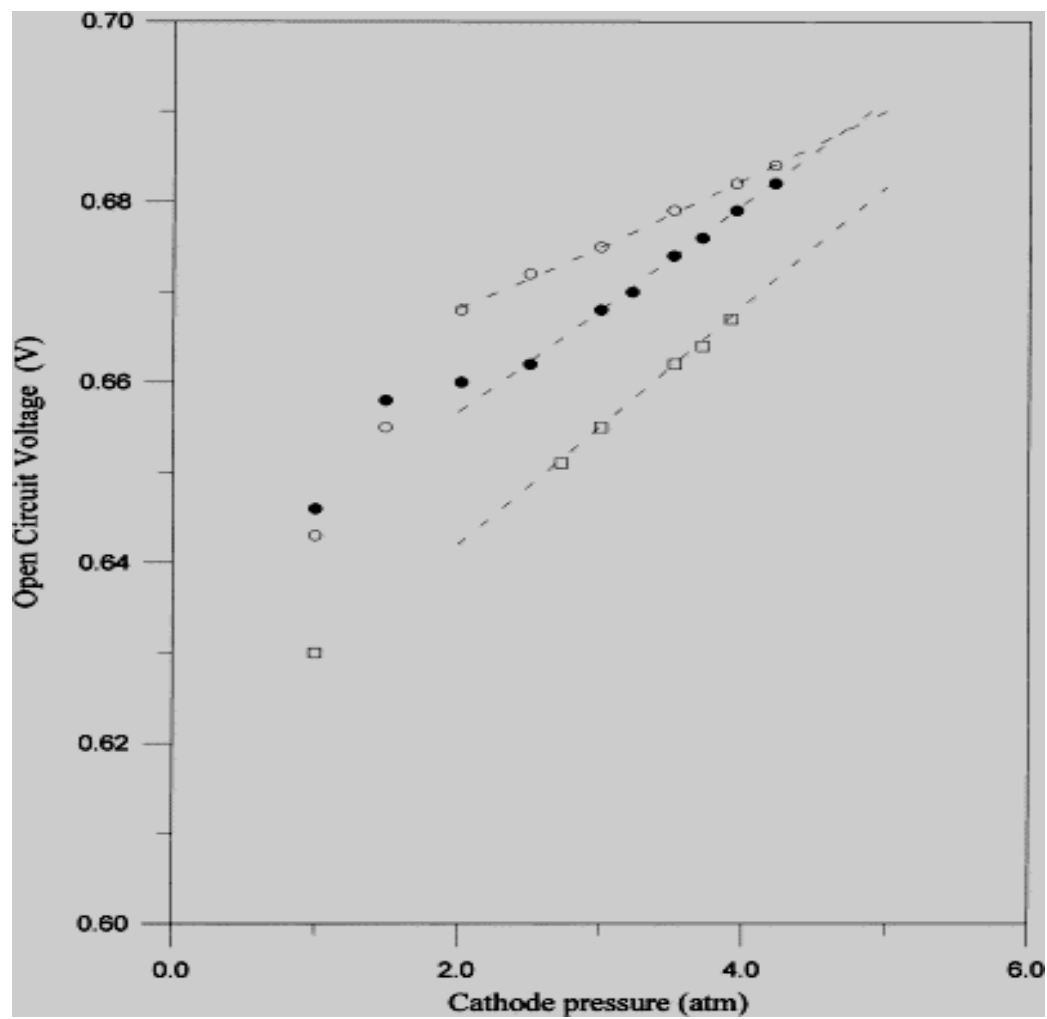


Figure 2-8: OCV as a function of the cathode pressure for Nafion 115 membrane at different DMFC operation times. The dotted lines correspond to the model equation; (○) first measurement; (●) second measurement; (□) third measurement.

Though OCV values are useful in determining membranes diffusivity care should be taken to make sure that correct values are recorded. When a cell is on load before it is put to the open circuit condition, the OCV jumps and reaches a peak in seconds. The voltage at this peak is just a transient value. After some minutes the voltage will drop until it stabilizes to a constant value which should be taken as the real OCV value [53].

2.5.3 Limiting Current Measurements

Methanol crossover fluxes can also be determined using diffusivity value of the membrane obtained by limiting current density measurements. If the methanol permeation is due to diffusion only, then the diffusivity is given as [58]:

$$D_m = \frac{J_{\text{lim}} l}{6FC_m} \quad (1)$$

D_m = membrane diffusivity, ($\text{cm}^2 \text{s}^{-1}$),

J_{lim} = Steady – state limiting current, (Acm^{-2})

Where l = membrane thickness, (cm)

F = Faraday constant, $96,484 \text{ Cmol}^{-1}$

C_m = CH_3OH concentration at the feed edge (M)

However, corrections for electro-osmotic drag effects are necessary even for low methanol concentrations; as such need to be taken into account for accurate methanol crossover flux measurement in a DMFC at open circuit voltage [58]. With the correction, the diffusivity becomes:

$$D_m = \frac{J_{\text{lim}} l}{6FC_m k_{dl}} \quad (2)$$

Where k_{dl} = drag correction factor for J_{lim}

2.5.4 Gas Chromatography (GC)

Gas chromatography is a non electrochemical technique that can be used to determine the concentration of the permeated methanol ($C_{B(t)}$) with time in the receiving compartment of a diffusion cell set-up. Normally, a capillary column in combination with a flame-ionization detector (FID) is used to determine the concentration of the methanol in the aqueous methanol solution after a certain crossover time. If the supporting electrolyte is aggressive, such as H_2SO_4 , then a HP-Innowax capillary column inserted in a GC using a FID should be used [64]. The technique apparently works fine, however the samples taken are prone to contamination before the GC analysis. Taking the samples to the GC for analysis also introduces additional work. However, if an online GC is available these problems will be resolved. But the presence of acidic electrolyte solution (H_2SO_4) needs a GC column that can withstand the acidic medium. In the DMFC, the permeated methanol oxidizes to CO_2 . Thus, relying on measuring the methanol concentration using GC is unsuitable when a real DMFC is used. Nevertheless, the technique could still be useful for preliminary screening of membranes in a diffusion cell set-up.

Similar to the gas chromatographic method where the methanol concentration of the receiving compartment ($C_{B(t)}$) is monitored with time, in a variation of this method the

receiving compartment is connected to a vacuum system that allows pervaporation of the crossed methanol [65]. The vaporized methanol is collected in cryogenic traps. This method could be cumbersome and like the gas chromatography is useful only for membranes screening since it does not simulate fuel cell conditions well.

2.5.5 Mass Spectrometry

Mass spectrometry of liquid samples of the cathode outlet stream is another way of determining the methanol crossover flux. For mass spectrometric measurements of methanol crossover, a clear description of the respective system could be achieved by measuring the background methanol signal of a cell filled with distilled water and equipped with the membrane sample, and subsequently adding well-adjusted portions of aqueous or pure methanol to this liquid. The slopes of mass signal vs. time curves are typical for diffusion-controlled processes and with the help of the calibration lines the diffusion coefficient of methanol through the membrane can be calculated. *Wang et al* [56] employed an on-line analysis of the cathode exhaust gas with multipurpose electrochemical mass spectrometry to determine the methanol crossover rates. They determined the methanol permeability for different water/methanol mole ratios fed to the anode and observed that the methanol crossover rate can be reduced by appropriate choice of water/methanol mole ratio. However, they made the assumptions that the entire permeated methanol gets converted to CO₂ and did not consider the anodic CO₂ contribution both of which can affect the results.

2.5.6 Cyclic voltammetry and chronoamperometry

Voltammetric and chronoamperometric techniques are widely used recently to determine the methanol crossover flux through polymer membranes intended for use in direct methanol fuel cell [52, 66-68]. These techniques can be used with either a real fuel cell or a simulated one (diffusion cell). In the diffusion cell set-up the methanol concentrations in the receiving compartment ($C_{B(t)}$) are obtained by recording the cyclic voltammograms (CVs) and chronoamperometric curves using AUTOLAB or EG & G PARC potentiostat/galvanostat with a programmable power supply. With these techniques the methanol diffusivity through the membrane can be studied both qualitatively and quantitatively. Figure 2-9 shows the permeability curves at different methanol concentration obtained by Ramya et al [66] using these methods. However, better results would be obtained if the methanol concentration in the receiving compartment is considered to be increasing with time instead of assuming it to be negligible especially when high initial methanol concentration is used in the reservoir compartment. They suggested an optimum concentration of 1-2 M solution for operation of fuel cells.

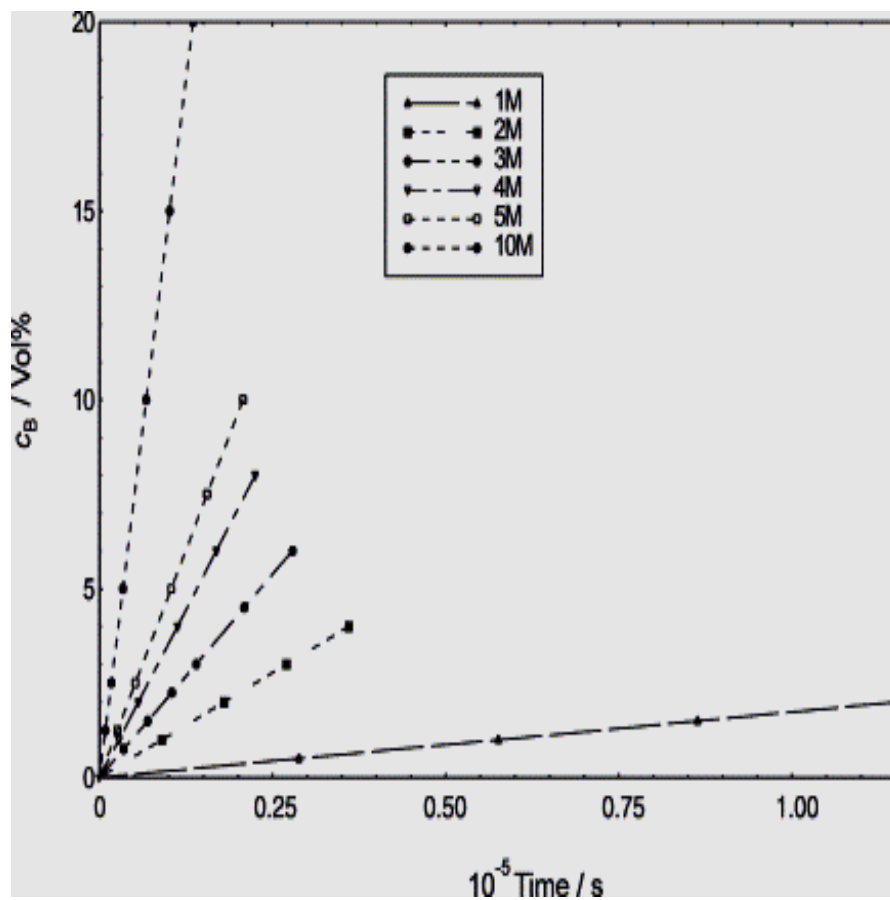


Figure 2-9: Permeability curves at various concentrations.

2.5.7 Potentiometric Technique

A potentiometric method has been developed for measuring methanol crossover and tested using Nafion membrane [69]. The slope $\left(\frac{dE}{dt}\right)$ of potential (E) versus time (t) curve was found to be proportional to the crossover rate. Figure 2-10 shows a plot of $\left(\frac{dE}{dt}\right)$ versus t (time), indicating higher crossover flux initially which reduces with time.

The potential (E) of a working electrode measured in the methanol receiving compartment has an inverse relationship with the methanol concentration. As such, the potential (E) values obtained with time can be used to determine the methanol concentrations ($C_B(t)$) as a function of time. Plot of ($C_B(t)$) versus time will give values of $\frac{dC_B}{dt}$. This slope will initially be high as the crossover starts but decreases as the flux reduces until it becomes zero at equilibrium concentration. An average methanol crossover flux can be obtained using flux relationship given as:

$$j_A = \frac{V_B}{A} \frac{dC_B}{dt} \quad (1)$$

Thus, the measurement of the electrode potential is useful in determining the methanol crossover flux across polymer electrolyte membranes.

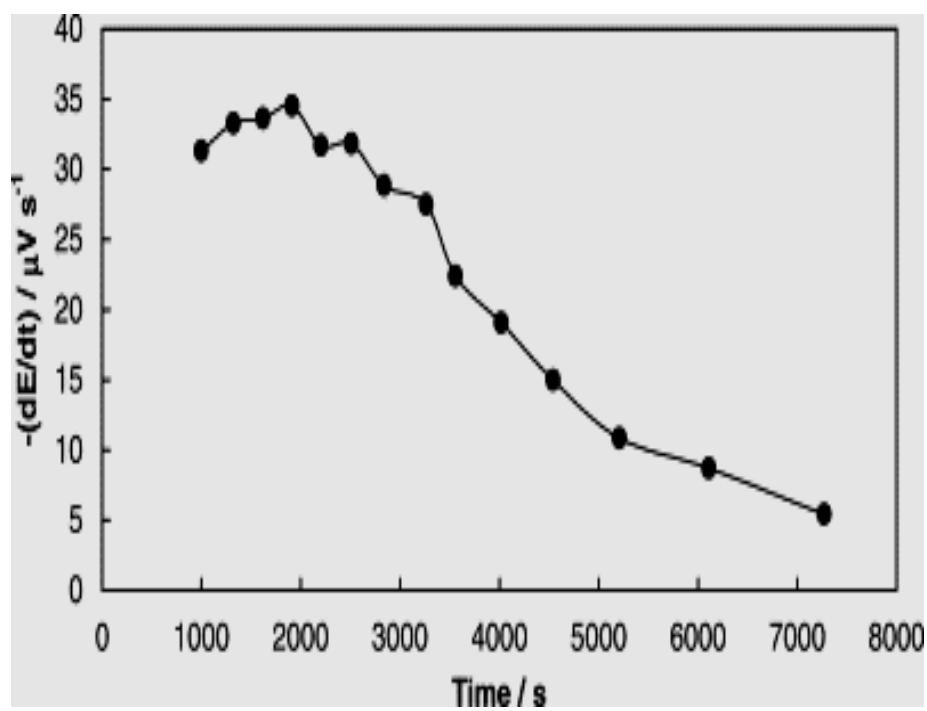


Figure 2-10: Variation of (dE/dt) during CH_3OH crossover

2.6 Working Electrode Positioning

In the diffusion cell study of the methanol crossover through polymer membranes the positioning of the working electrode is very important. The best way is to attach the working electrode on the membrane or to prepare it on the membrane by suitable method; such as electroless deposition. Nanosize Pt electrode prepared by electroless deposition can be used as the working electrode for the electrochemical techniques [52]. Attaching the electrode on the membrane enhances the methanol oxidation current detection and gives the actual flux value without any effect of mass transfer resistance encountered when the electrode is placed somewhere in the bulk solution away from the membrane surface. Even small distance away from the membrane surface; say 100 μm , can affect the results because the methanol oxidation current may not be detected [67]. Thus, the working electrode should be placed appropriately for accurate results.

One of the challenges of using Pt electrode in determining methanol permeability of membranes by electrochemical oxidation method is poisoning. The Pt could be poisoned by the CO produced as an intermediate during the dehydrogenation process. Pt-Ru catalyst is more suitable because Ru can dissociate water at lower potentials to create oxygen-containing surface groups that are needed to convert CO to CO_2 [53].

CHAPTER 3

3 EXPERIMENTAL SET-UP AND PROCEDURE

3.1 Methanol Permeability Determination

3.1.1 Cell Design and Experimental Set-up

A schematic diagram of a two-compartment diffusion cell fabricated for the experiments is shown in Figure 3-1. Each compartment has a volume of about 220ml. The compartments have a provision to put a working electrode, reference electrode, counter electrode and a stirrer. The prepared diffusion cell was connected to a potentiostat as shown in Figure 3-2 in order to conduct the measurements. Three electrochemical techniques; cyclic voltammetry, chronoamperometry, and potentiometry were conducted experimentally. The procedure of each one of them is described in this section.

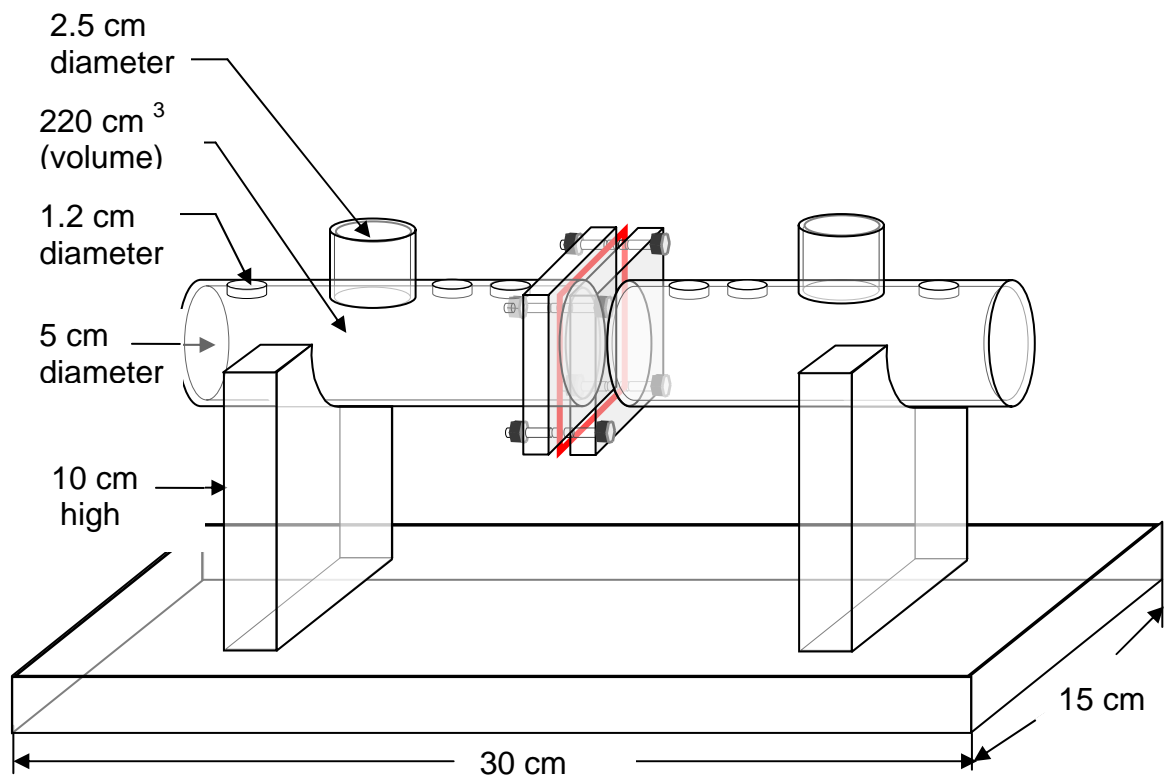


Figure 3-1: Schematic Diagram of the Fabricated Cell

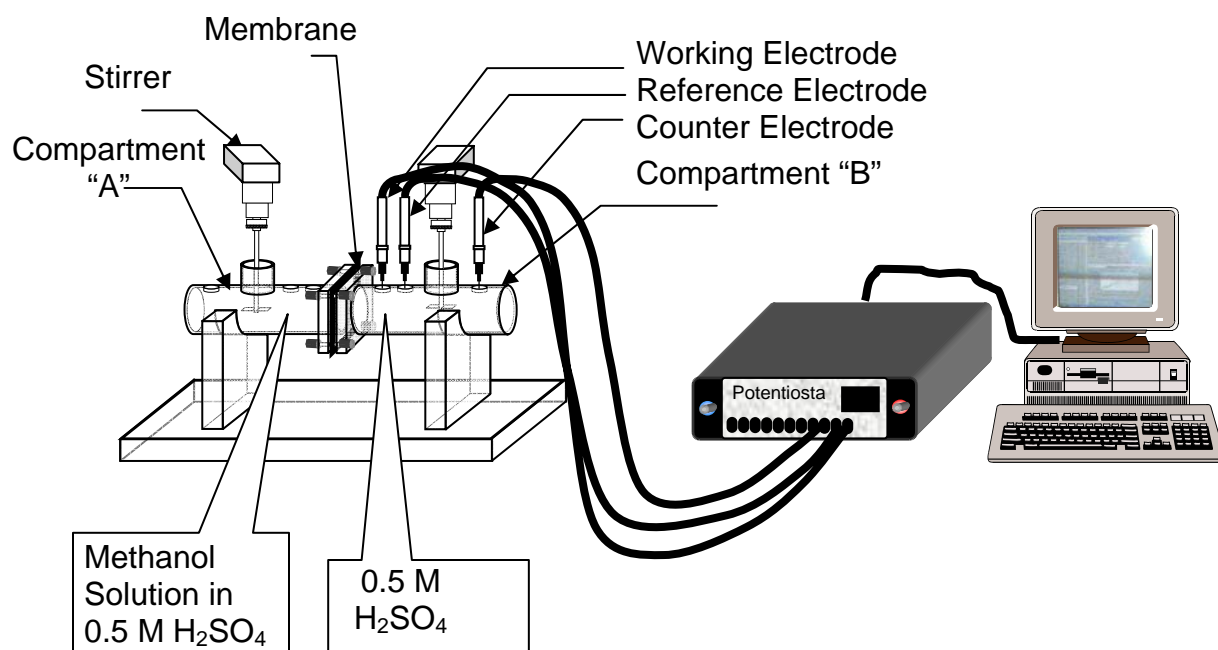


Figure 3-2: Experimental Set-up

3.1.2 Procedure for Cyclic Voltammetry

The two-compartment diffusion cell set-up was used to determine the permeability of Nafion[®] 117 membrane in methanol solutions. The Nafion[®] 117 membranes (DuPont) of 0.18mm thickness was first treated with 3% hydrogen peroxide solution, distilled water, 0.5M sulfuric acid solution successively, and stored in distilled water. A membrane of an area of 13.85 cm² was placed between the two compartments by a screw clamp. Each cell of about 220ml capacity has a provision to introduce the working electrode (Pt wire), counter electrode (Pt foil), reference electrode (Saturated Calomel Electrode, (SCE)), and a stirrer. An experiment was started by putting 110ml of deoxygenated supporting electrolyte (0.5M H₂SO₄) into each of the compartments. Then 110ml of deoxygenated methanol solution of known concentration was added to the reservoir compartment (cell A) and an equal volume of distilled water was added to the receiving compartment (cell B) to maintain equal hydrostatic pressure, and also equal concentration of the supporting electrolyte on both sides of the membrane. All the three electrodes were put in the cell where readings were to be taking. The working electrode (Pt wire) is placed as close to the membrane as possible. CVs were recorded using AUTOLAB Potentiostat (GPES). Potential limits of -0.25V to 1.2V, with step increase of 0.003mV were used. The experiments were carried out at 21 ± 2 °C.

3.1.3 Procedure for Chronoamperometry

The same procedure like in the cyclic voltammetric technique was used for the chronoamperometric technique except that in the chronoamperometry a single value potential was given. From the cyclic voltammograms, it was established that the methanol oxidation takes place at 0.65V vs. SCE which agrees with the literature value reported. This potential (0.65V) was used in the chronoamperometry to determine the current generated due to the methanol oxidation at the Pt electrode in the receiving compartment. Methanol concentrations were determined using the concentration vs. current calibration curve.

3.1.4 Procedure for Potentiometric Technique

Just like in the cyclic and chronoamperometric techniques the same diffusion cell set up and procedure were used for the potentiometric technique except that instead of recording CVs or chronoamperometric curves, potential (E) was recorded versus time (t). The experiment was started by taking 110ml of deoxygenated 0.5M H_2SO_4 (supporting electrolyte) into both the reservoir and receiving compartments. All the three electrodes were put in the receiving compartment with careful placement of the working electrode (Pt wire) as close to the membrane as possible. The potential of the Pt wire (working electrode) in 0.5M H_2SO_4 was monitored for an hour to ensure a stable value, which is about 0.52V vs. SCE. Then 110ml of deoxygenated methanol solution of known concentration was added to the reservoir compartment (cell A) and equal volume of distilled water was added to the receiving compartment (cell B) to maintain equal hydrostatic pressure, and equal concentration of the supporting electrolyte on both sides

of the membrane. While stirring the reservoir compartment, the potential of the Pt wire electrode in the receiving compartment was recorded during the permeation period using AUTOLAB Potentiostat/galvanostat (GPES). After methanol reaches the receiving compartment, the Pt electrode senses the methanol and its potential tends to shift. Methanol concentrations were obtained using the potential vs. concentration calibration curve. The experiments were carried out at 21 ± 2 °C.

3.2 Composite Membranes Preparation

3.2.1 Loading of Tungstonphosphoric acid onto MCM-41 and Y-zeolite

Loading of the tungstonphosphoric acid (TPA) onto MCM-41 or Y-zeolite and preparation of the composite membranes were carried out as described in the literature [6]. A known amount of TPA was dissolved in distilled water and few drops of dilute hydrochloric acid (HCl) added in order to avoid hydrolysis of the TPA. Then required amount of MCM-41 or Y-zeolite was added to make a suspension, followed by sonification for 30 minutes. The suspension was then heated at around 80 °C to 100 °C while stirring until all the water was evaporated to obtain a concentrated solid material which was dried in an oven at 200 °C for 5hrs. The concentrated material was then grounded into fine powder and stored in a glass tube for use. The TPA/ MCM-41 or Y-zeolite powder particles were made very fine in order to have good dispersion into the polymer matrix (SPEEK).

3.2.2 Membranes Preparation

Solution casting method, which is normally used for preparing dense polymeric materials, was used in preparing the composite membranes. A known amount of SPEEK 1.6 IEC was dissolved in dimethylacetamide (DMAc, 99% grade) and required amount of the MCM-41 or TPA/Y-zeolite material was added to make a suspension. While stirring, the suspension was heated at 100 °C -140 °C for about 5 hrs until most of the solvent (DMAc) was evaporated and a viscous mixture was obtained. The viscous mixture was then cast onto a flat glass plate and spread using a casting knife. The cast membranes were dried at ambient temperature and then, at around 80°C in an oven.

3.3 Determination of Methanol Permeability of the SPEEK/TPA/ MCM-41 or Y-zeolite Composite Membranes

Potentiometric technique was used in determining the methanol permeability of the SPEEK/TPAs/Y-zeolite or MCM-41 composite membranes. The membranes were pretreated with 3% hydrogen peroxide solution, distilled water, 0.5M sulfuric acid solution successively, and stored in distilled water. They are stable up to 150 °C in the acidic medium. The procedure described in section 3.1.2 was exactly followed to record the potential (E) values versus time (t) which were converted to concentrations using the potential vs. concentration calibration curve.

CHAPTER 4

4 RESULTS AND DISCUSSION

4.1 Determination of Methanol Permeability of Nafion® 117 Membrane

Five techniques for determining methanol permeability of proton exchange membranes were considered and evaluated in this work. Monitoring CO₂ content at the cathode exhaust of DMFC and measuring concentration of the diffused methanol using gas chromatography (GC) were found to have inherent drawbacks (as contained in the literature review) that make them unsuitable. Cyclic voltammetry, chronoamperometry and potentiometric techniques were conducted experimentally.

These techniques rely on measuring current density or potential values which can be converted to methanol concentration. Theoretically, the concentration, flux and permeability relationship can be derived using a simple sketch of a two- compartment diffusion cell (Figure 4-1), and some mass transfer equations.

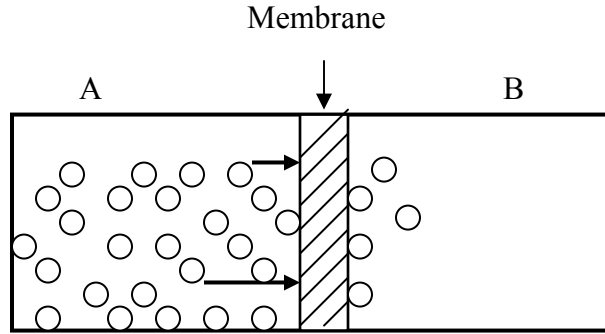


Figure 4-1: Schematic of methanol crossover through a membrane from reservoir compartment (A) to receiving compartment (B).

Unsteady state material balance on the receiving compartment (B) yields;

$$j_A = \frac{V_B}{A} \frac{dC_B}{dt} \quad (1)$$

Where;

j_A = Methanol flux from the reservoir compartment (A) to receiving compartment (B)

V_B = Volume of compartment B

A = Membrane area

C_B = Methanol concentration in the receiving compartment

t = Time

Simplified expression for Fick's law is given as;

$$j_A = \frac{DK}{l} (C_A - C_B) \quad (2)$$

Where;

D = Methanol diffusivity (assumed to be constant inside the membrane)

K = Partition coefficient (constant).

DK = Membrane permeability.

l = Membrane thickness

C_A = Methanol concentration in the reservoir compartment

Combining equation (1) and (2) gives:

$$V_B \frac{dC_B}{dt} = A \frac{DK}{l} (C_A - C_B) \quad (3)$$

Taking methanol molar balance for the two compartments gives;

$$C_{A_0} \times V_A = C_A \times V_A + C_B \times V_B \quad (4)$$

Assuming $V_A \approx V_B$ always, then:

$$V_B \frac{dC_B}{dt} = A \frac{DK}{l} (C_{A_0} - 2C_B) \quad (5)$$

Thus,

$$\int_{C_{B_0}}^{C_{B(t)}} \frac{1}{C_{A_0} - 2C_B(t)} dC_B = A \frac{DK}{V_B l} \int_{t_0}^t dt \quad (6)$$

This simplifies to;

$$-\ln\left(1 - \frac{2C_B(t)}{C_{A_0}}\right) = 2A \frac{DK}{V_B l} (t - t_0) \quad (7)$$

Where;

$$\frac{C_{A_0}}{C_{B(t)}} > 2$$

If $C_B(t)$ is known, then from the slope of linear plot of equation (7), the permeability (DK) of the membrane could be obtained. An average methanol crossover flux can be determined using $\frac{dC_B}{dt}$ values and equation (1). $C_B(t)$ is expressed as follows:

$$C_B(t) = \frac{C_{A_0}}{2} \left[1 - e^{-\frac{2ADK}{V_B l}(t-t_0)} \right] \quad (8)$$

From equation (3), if $C_A(t) \gg C_B(t)$, then:

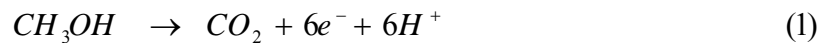
$$C_B(t) = \frac{ADK}{V_B l} C_{A_0} (t-t_0) \quad (9)$$

C_{iA_0} = Methanol initial concentration in the reservoir compartment,

t_0 = Time lag related to diffusivity as $t_0 = \frac{L^2}{6D}$.

4.1.1 Cyclic Voltammetry

Cyclic voltammetry is an electrochemical technique that can be used to study methanol crossover both qualitatively and quantitatively. It is expected that the only electron transfer reaction which can occur at the working electrode surface, within the potential range under consideration, is the methanol oxidation.



$$\text{Rate of oxidation} = k (C_{CH_3OH})_{\text{at the electrode surface}} \quad (2)$$

Based on the established theoretical relationship between current density and concentration of reactant species (methanol in this case), the cyclic voltammetric technique has been used by many researchers to determine methanol permeability of proton exchange membranes. This technique is employed here. Figure 4-2 shows voltammograms obtained for different methanol concentrations at a scan rate of 100mV/s. As can be observed, the methanol oxidation current peak increases with increasing methanol concentration. The oxidation current peak values were plotted against the methanol concentration as shown in Figure 4-3, to obtain a calibration curve. The calibration curve was then used to convert measured current densities in both the reservoir compartment (A) and the receiving compartment (B) to methanol concentrations.

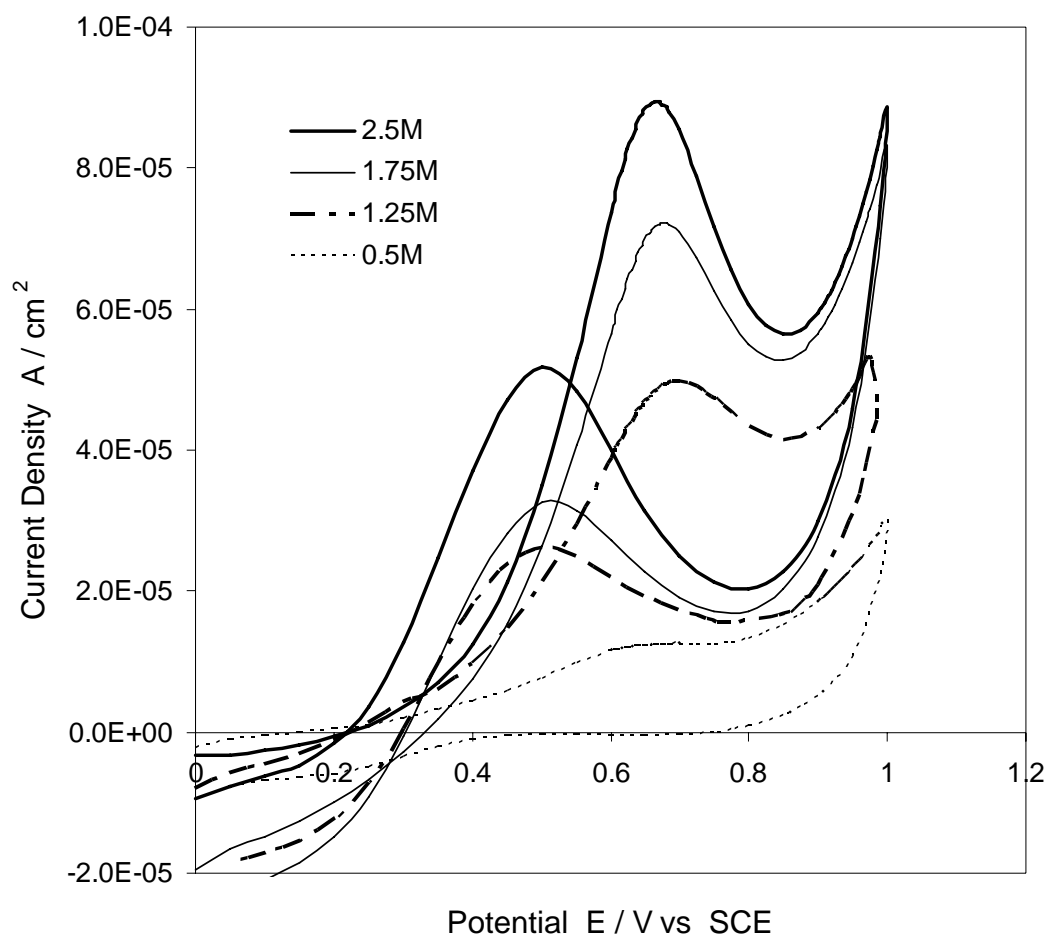


Figure 4-2: cyclic voltammograms at a scan rate of 100mV/s for different methanol concentrations.

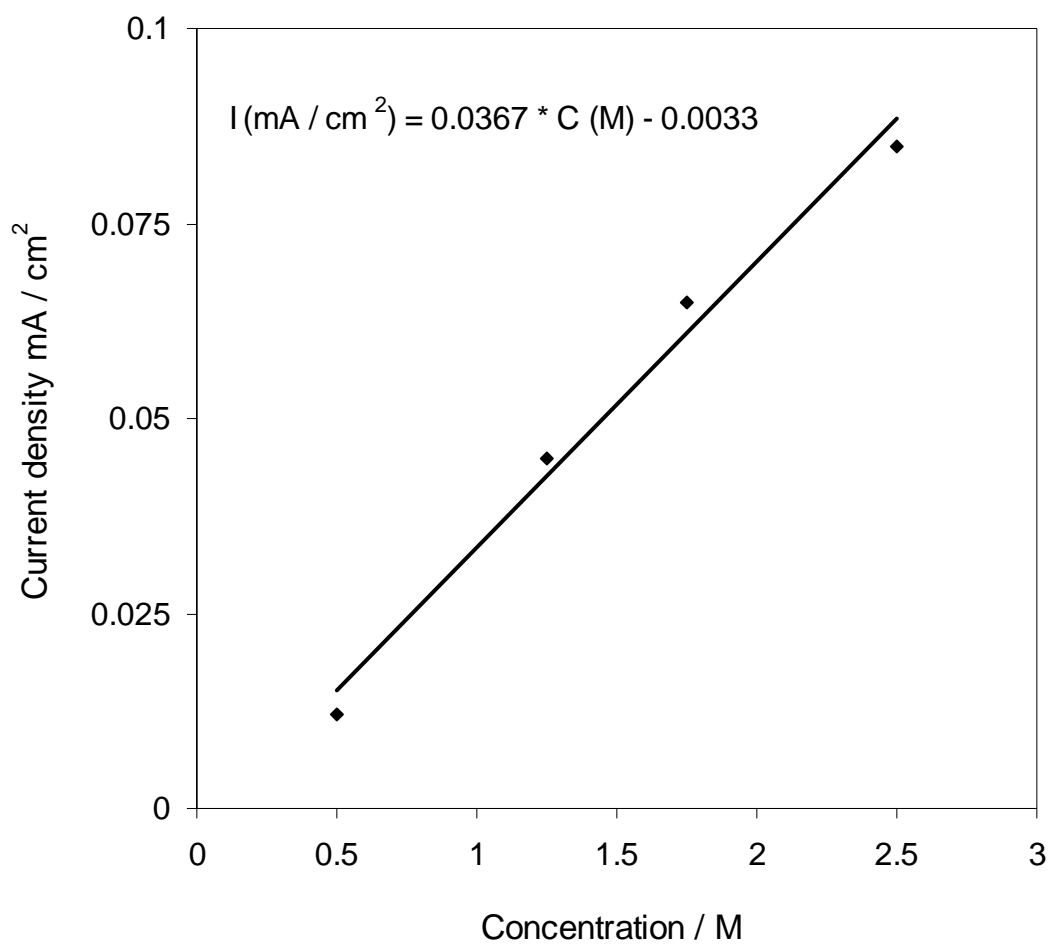


Figure 4-3: Calibration curve for the cyclic voltammetry.

Having done the calibration for the current density against the methanol concentration, the experiment was then conducted to determine the methanol crossover flux of Nafion[®] 117 membrane. The Nafion[®] 117 membrane was placed between the two compartments and the procedure for the cyclic voltammetry mentioned in section 3.1.1 was followed.

However, during the experiment the methanol oxidation current peaks for the receiving compartment could not be detected immediately. This could be expected because the working electrode was placed somewhere in the bulk solution a little bit away from the membrane surface. Attaching the electrode on the membrane surface enhances the methanol oxidation current peak detection and reduces the effect of mass transfer resistance. It has been reported that methanol oxidation current peak may not be detected even for a small distance away from the membrane surface [67]. Thus, the positioning of the working electrode is very important. The best way is to attach the working electrode on the membrane or to prepare it on the membrane by suitable method; such as electroless deposition [52].

Nevertheless, using the methanol molar balance expression for the two compartments (equation 4), concentrations for the receiving compartment C_B can be obtained if the concentrations in the reservoir compartment C_A are known. Figure 4-4 shows voltammograms obtained for the methanol reservoir compartment (side A) at different time periods for 2.5M initial methanol concentration. It can be seen that, the methanol oxidation current peak decreases with time indicating the loss of methanol due to the crossover to the receiving compartment (side B).

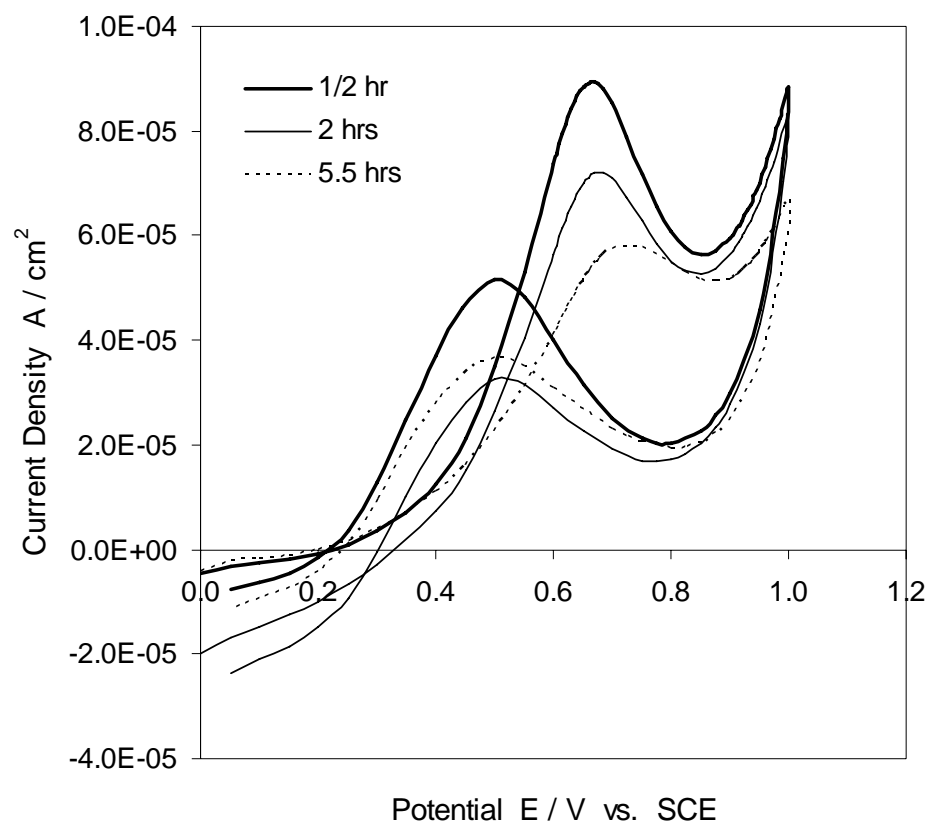


Figure 4-4: Cyclic voltammograms at a scan rate of 100mV/s for the reservoir compartment (side A) at different time for 2.5M initial methanol concentration.

The methanol molar balance expression (equation 4) was used to obtain the concentration values for the receiving compartment C_B . These values and the model equation (equation 7) were used to make a linear plot, Figure 4-5. The slope of the plot is related to the membrane permeability.

Using the model equation;

$$-\ln\left(1 - \frac{2 \cdot C_B(t)}{2.5}\right) = 2 \frac{ADK}{V_B l} (t - t_0)$$

Where $A = 13.85 \text{ cm}^2$, $V_B = 220 \text{ cm}^3$, $l = 0.02 \text{ cm}$, and $\text{slope} = 8 \cdot 10^{-6} / \text{s}$

This implies;

$$\text{Permeability } (DK) = 1.27 \times 10^{-6} \text{ cm}^2 \text{ s}^{-1}$$

In the cyclic voltammetry, the methanol oxidation current peak varies with the scan rate as shown in Figure 4-6. This implies that researchers using different scan rates will observe diverse current readings resulting in varying concentration values. This would result in reporting different permeability and crossover flux values. Thus, in order to use cyclic voltammetric technique accurately for concentration determination, a constant scan rate has to be maintained throughout the experiment.

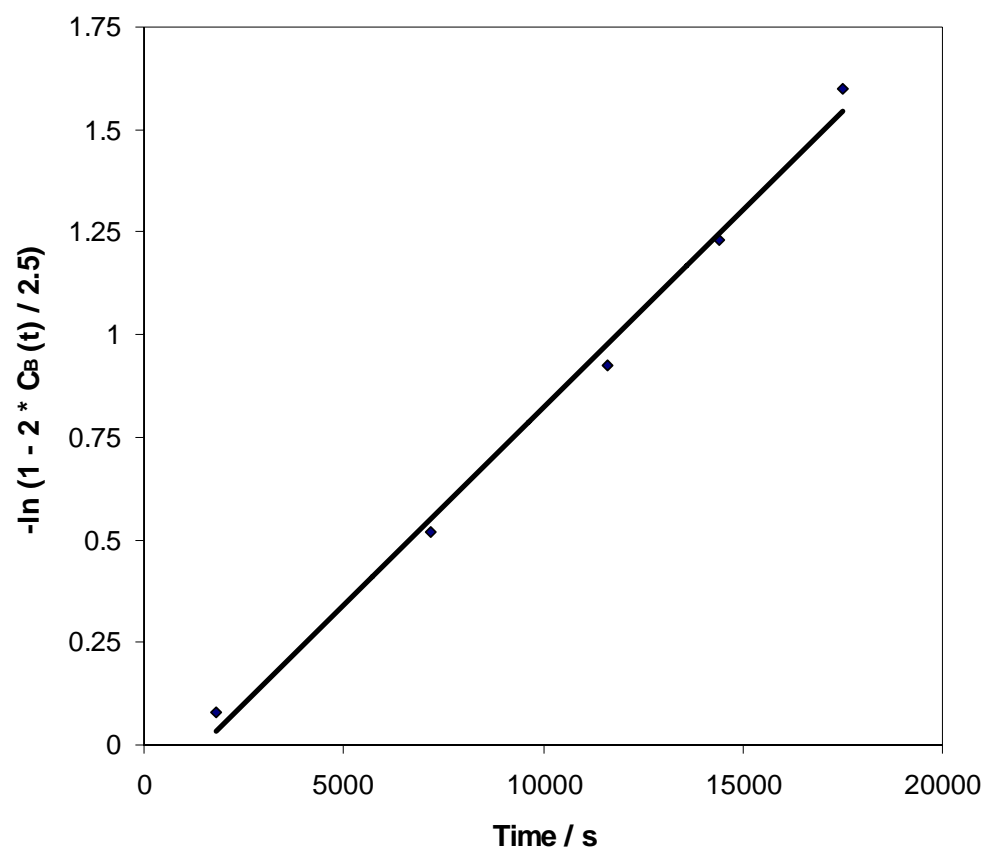


Figure 4-5: Plot of concentration model equation vs. time for an initial methanol concentration of 2.5M.

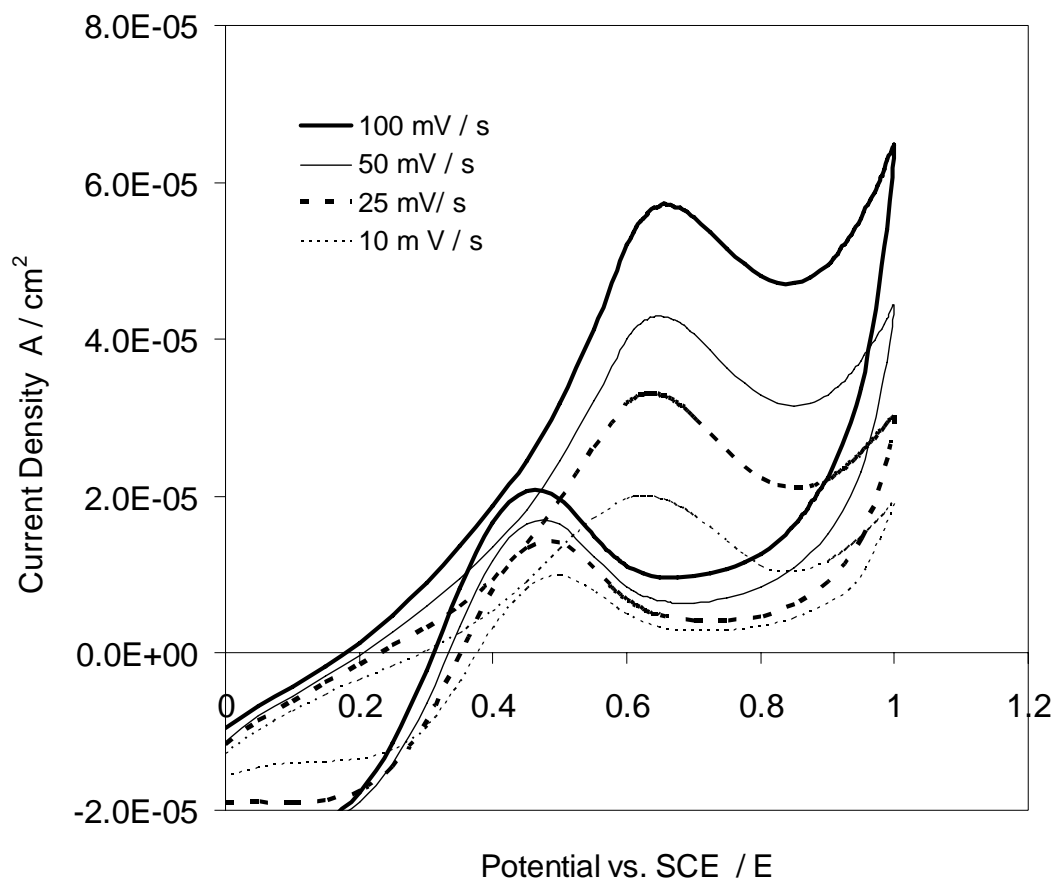


Figure 4-6: Cyclic voltammograms at different scan rates after 6 hrs for the receiving compartment (Side B) for 2.5M initial methanol concentration in the reservoir compartment.

4.1.2 Chronoamperometry

Just like in the cyclic voltammetry, a calibration of current density against methanol concentrations was first determined. In the chronoamperometric experiment, a single value potential was given and current readings of both the reservoir and the receiving compartments were recorded at various time intervals. It has the same theoretical foundation with the cyclic voltammetry. In all the voltammograms it can be observed that the oxidation current peaks appeared at around 0.65V potential Vs SCE, which is similar to the value reported in the literature [69]. This potential (0.65V) was used in the chronoamperometry to determine the current generated due to the methanol oxidation at the Pt electrode in the two compartments with time. The current readings taken were then converted to methanol concentrations using the calibration curve. Chronoamperometry has the advantage of being applicable even when small concentrations are to be determined. Figure 4-7 shows chronoamperometric curves for different methanol concentrations at 0.65V vs. SCE.

It can be observed that the current density increases with increasing methanol concentration just like in the cyclic voltammetric technique. The current density values were plotted against the methanol concentration as shown in Figure 4-8, to obtain a calibration curve. The calibration curve was then used to convert measured current densities in both the reservoir compartment (A) and the receiving compartment (B) to concentrations

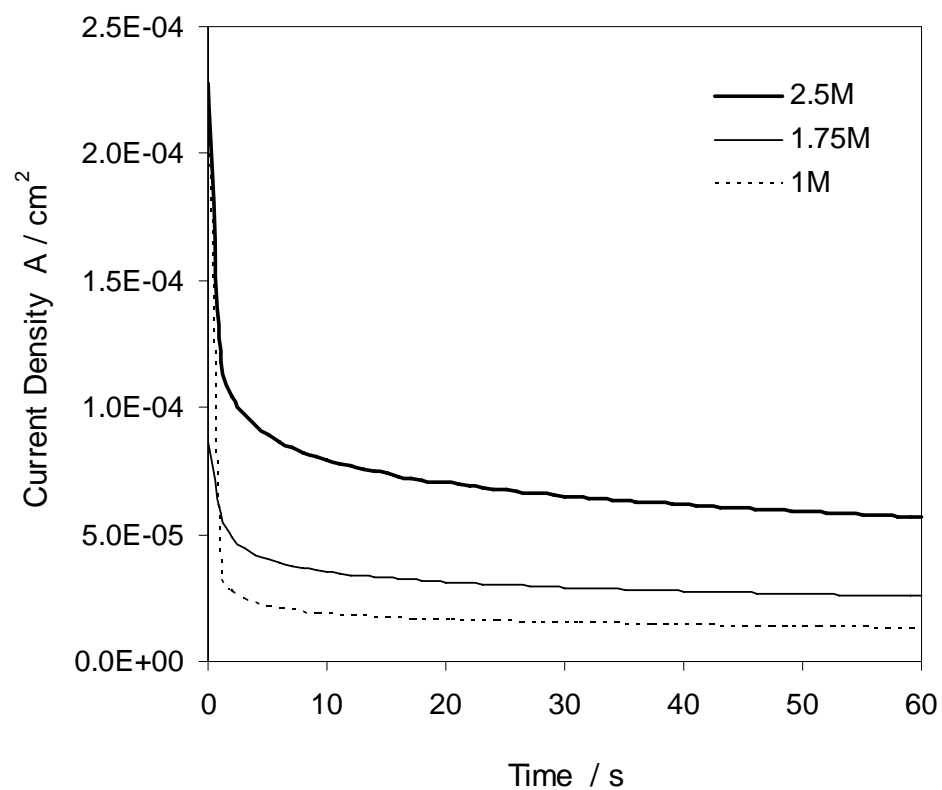


Figure 4-7: Chronoamperometric curves for the methanol oxidation at 0.65V vs. SCE for different concentrations.

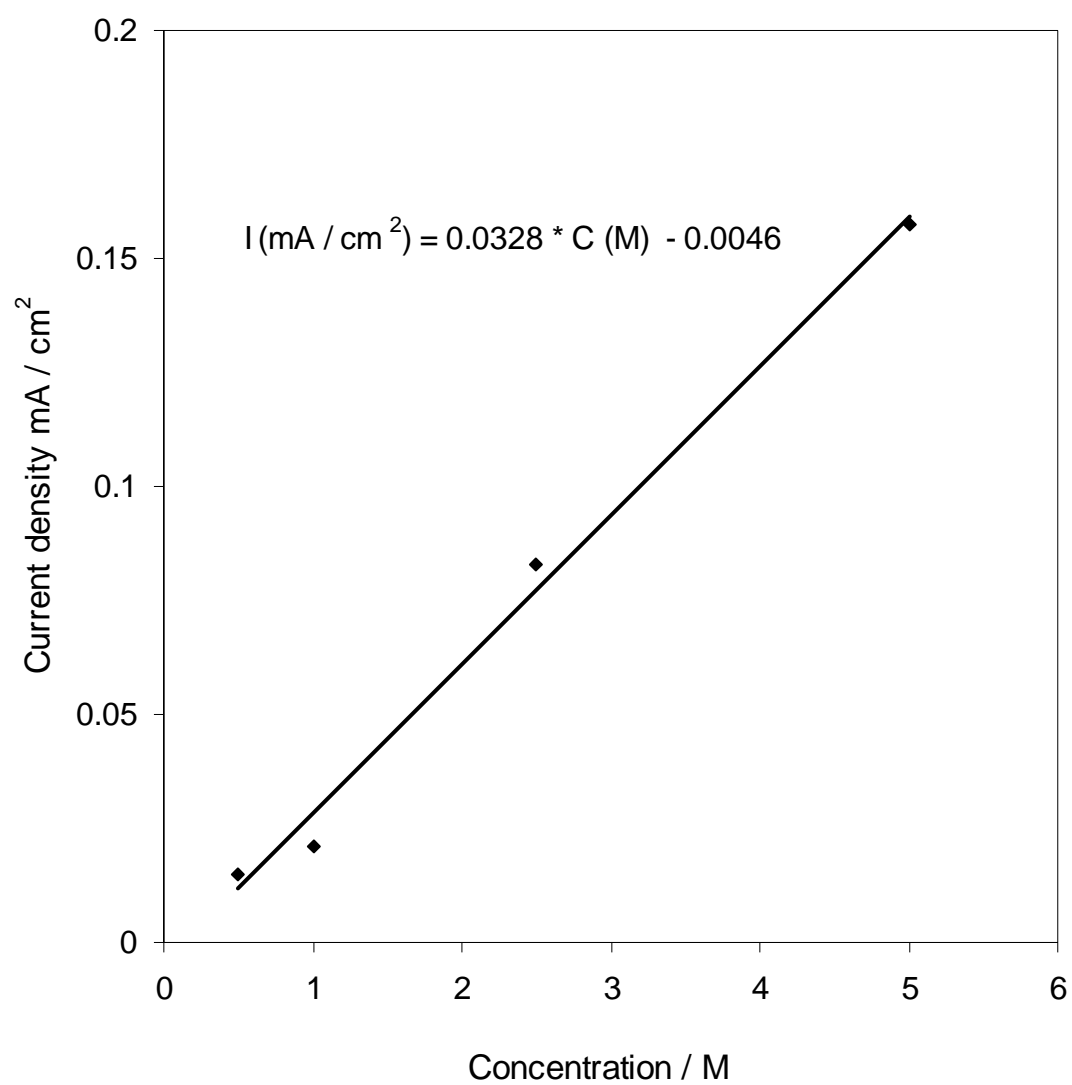


Figure 4-8: Calibration curve for the chronoamperometry.

Chronoamperometric curves showing the methanol oxidation current for the receiving compartment (side B) for an initial methanol concentration of 2.5M at different times are shown in Figure 4-9. It can be observed that the current density increases with time indicating increasing methanol concentration in the receiving compartment. Also, chronoamperometry curves for both the reservoir compartment (side A) and the receiving compartment (side B) are shown in Figure 4-10. The chronoamperometry curves for the reservoir compartment show decrease in the current density with time indicating loss of methanol. While the curves for the receiving compartment show rise in the current density with time corresponding to increase in the methanol concentration in that compartment. The obtained concentration values for the receiving compartment and the model equation (equation 7) were used to make a linear plot as shown in Figure 4-11.

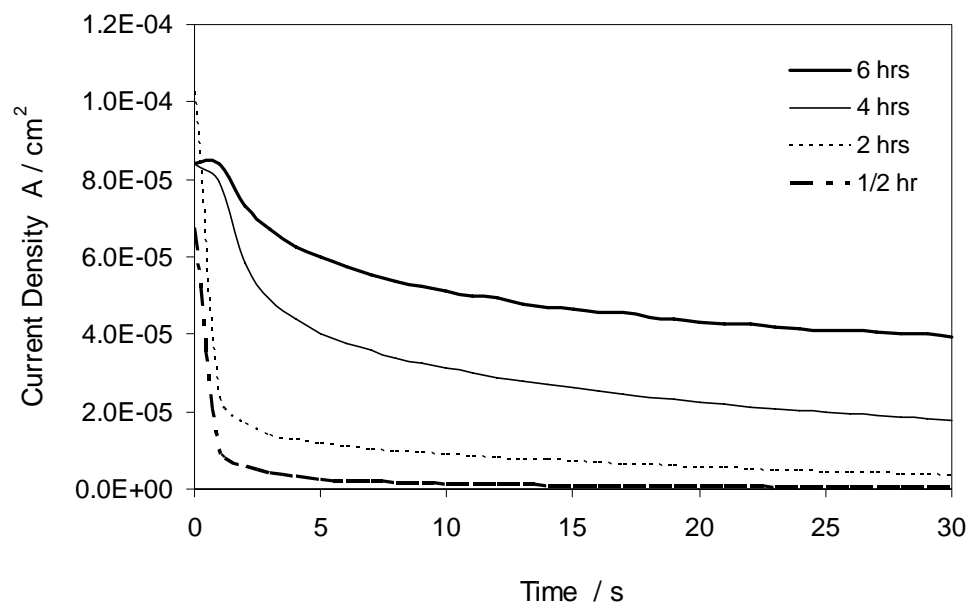


Figure 4-9: Chronoamperometry curves at 0.65V vs. SCE for the receiving compartment (side B) at different time for 2.5M initial methanol concentration.

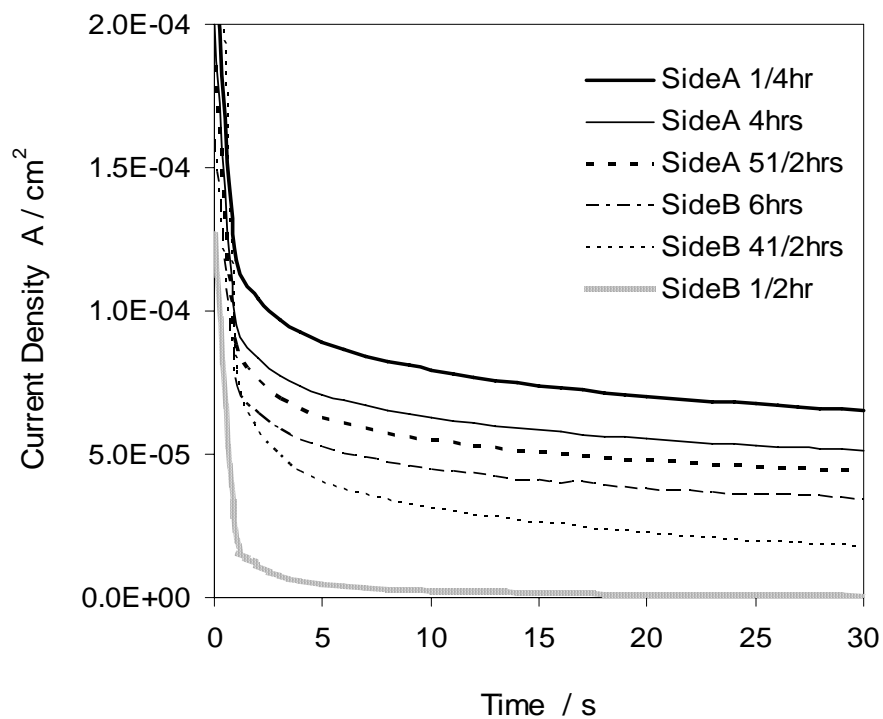


Figure 4-10: Chronoamperometry curves for both the reservoir compartment (side A) and the receiving compartment (side B) at different time for 2.5M initial concentration.

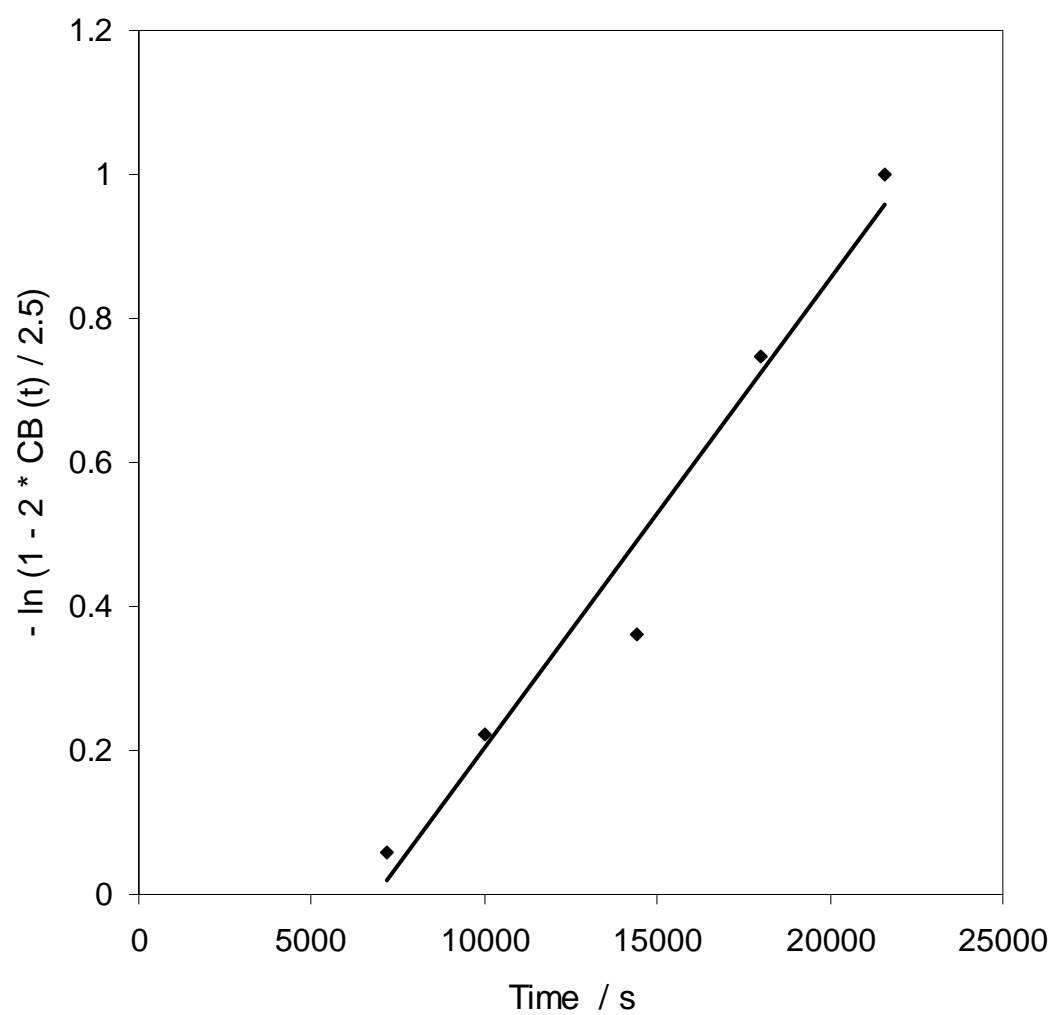


Figure 4-11: Plot of concentration model equation vs. time for an initial methanol concentration of 2.5M.

Using the model equation;

$$-\ln\left(1 - \frac{2*CB(t)}{2.5}\right) = 2 \frac{ADK}{V_B l} (t - t_0)$$

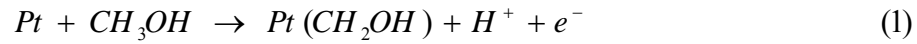
Where $A = 13.85 \text{ cm}^2$, $V_B = 220 \text{ cm}^3$, $l = 0.02 \text{ cm}$, and $\text{slope} = 7*10^{-6} / \text{s}$

This implies;

$$\text{Permeability } (DK) = 1.11 \times 10^{-6} \text{ cm}^2 \text{ s}^{-1}$$

4.1.3 Potentiometric Technique

The mechanism of electro-oxidation of CH_3OH is complex in nature because the reaction involves a transfer of six electrons resulting in mixed potential. Dissociative adsorption of CH_3OH on the electrode surface is assumed to be the important step in the mechanism. Thus, equilibrium is assumed to be established at the Pt electrode;



Nernst equation relates the potential (E') of reaction (1) to concentration as follows [69]:

$$E' = E^0 - \left(\frac{RT}{F}\right) \ln\left(\frac{C_B}{\theta_{ad} C_{H^+}}\right) \quad (2)$$

E^0 is the standard electrode potential and θ_{ad} the surface coverage by the adsorbed species. Expressing equation (2) in terms of C_B gives:

$$C_B = \theta_{ad} C_{H^+} \exp\left(F \frac{E^0 - E'}{RT}\right) \quad (3)$$

This gives;

$$\frac{dC_B}{dt} = -k' \exp\left(F \frac{E^0 - E'}{RT}\right) \left(\frac{dE'}{dt}\right) \quad (4)$$

To arrive at equation (4), θ_{ad} and C_{H^+} were considered constant and an empirical constant k' ($\text{mol V}^{-1} \text{l}^{-1}$) is introduced to balance the equation with respect to dimensions.

Equation (4) can be related to the crossover flux using;

$$J_A = \frac{V_B}{A} \frac{dC_B}{dt} \quad (5)$$

Combining (4) and (5) yields;

$$j_A = \left(\frac{V_B k'}{A}\right) \exp\left(F \frac{E^0 - E'}{RT}\right) \left(\frac{dE'}{dt}\right) \quad (6)$$

Thus, Nernst equation provides the theoretical foundation for this technique.

For the potentiometric technique, the variation of the open circuit potential (E) of the Pt electrode (working electrode) in the receiving compartment was monitored during the CH_3OH crossover. To determine the concentrations corresponding to measured potential values, calibration was made by measuring the potential of the Pt electrode in $0.5M H_2SO_4$ containing CH_3OH of different concentrations. Calibration plot is shown in Figure 4-12, with a slope of 0.0557 which is similar to the Nernstian slope value of 0.0592 V at 25°C.

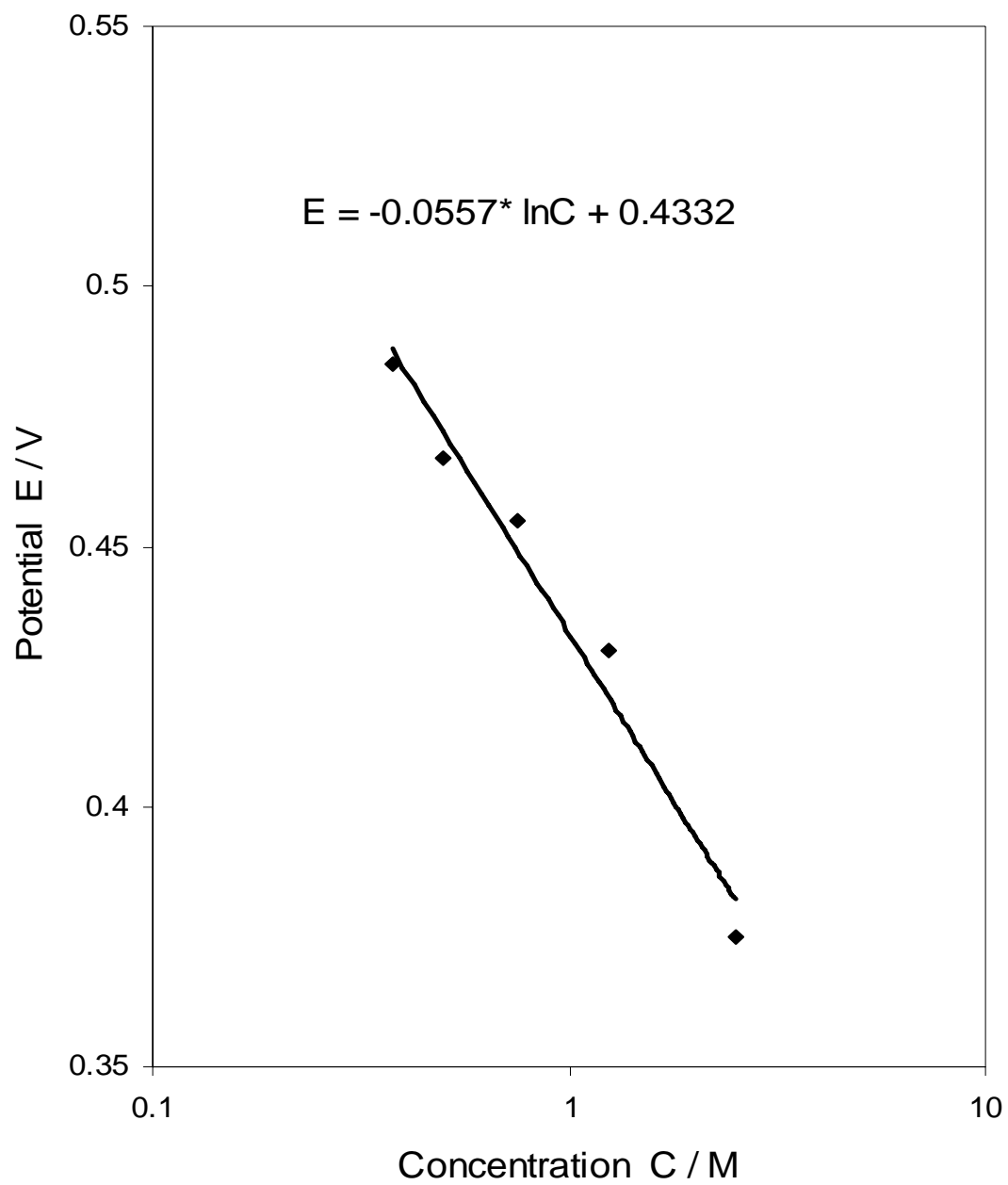


Figure 4-12: Calibration for the Potentiometry.

Potentiometric curves obtained when 5M, 2.5M and 1M initial methanol concentrations were introduced in the reservoir compartment and the potential of the Pt electrode in the receiving compartment monitored with time are shown in Figure 4-13. It can be observed that, the higher the initial methanol concentration in the reservoir compartment the less the potential values. The potential values measured with respect to time were converted to concentrations with the help of the calibration curve. Figure 4-14, shows increase in methanol concentration with respect to time for the receiving compartment for different initial methanol concentrations in the reservoir compartment. As expected, when high initial concentration in the reservoir compartment was used, early detection of the methanol in the receiving compartment and a steeper slope were observed.

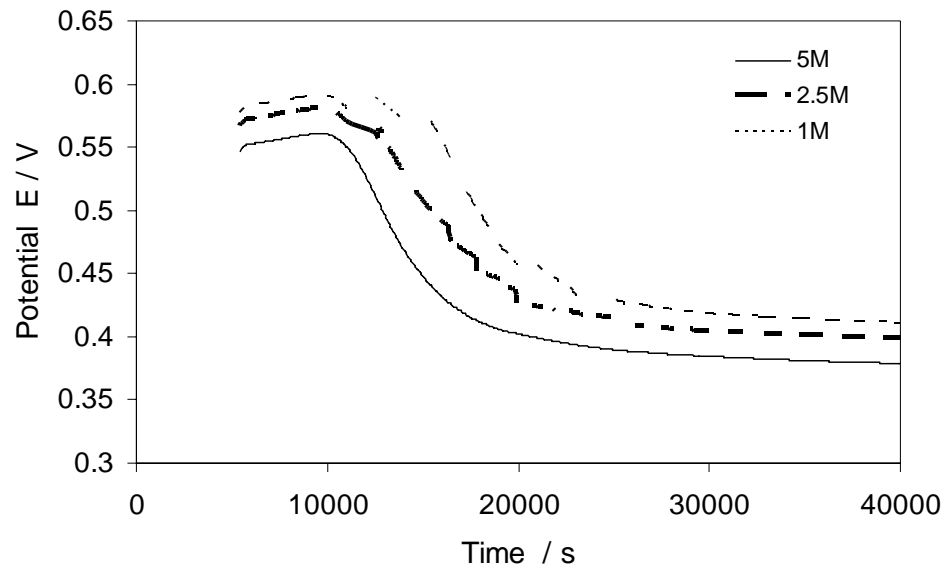


Figure 4-13: Potentiometric curves for the receiving compartment for different initial methanol concentration in the reservoir compartment.

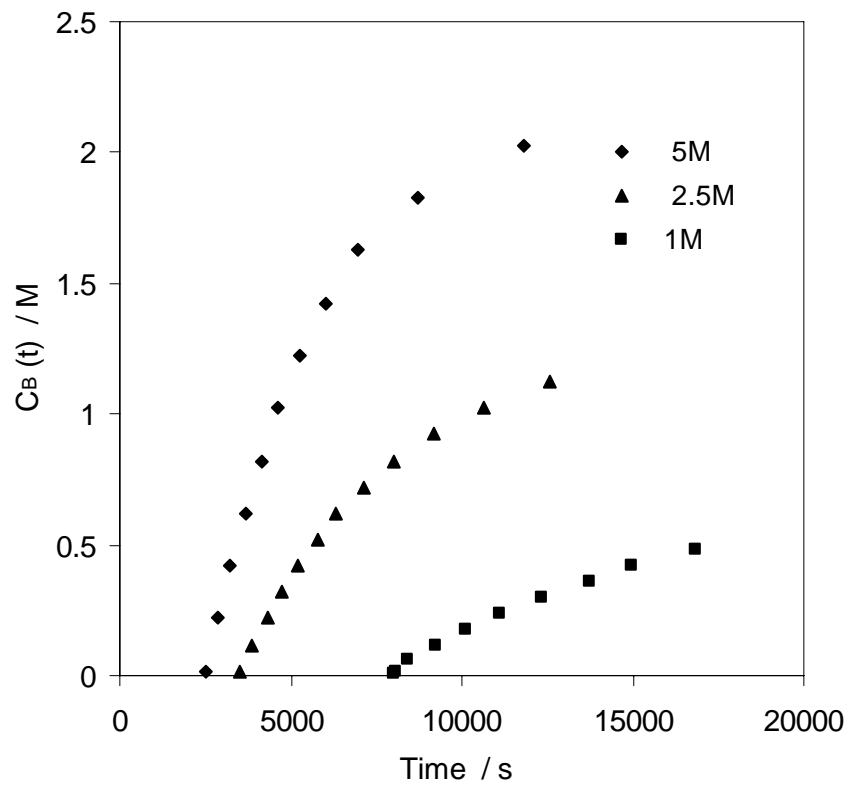


Figure 4-14: Methanol concentrations in the receiving compartment during crossover for different initial methanol concentrations in the reservoir compartment

In order to determine methanol crossover flux, concentration values for the receiving compartment for 2.5M initial concentration in the reservoir compartment were plotted against time and the following equation was obtained:

$$C_B(t) = 0.6313 * \ln(t) - 5.6518 \quad (7)$$

which gives;

$$\frac{dC_B}{dt} = \frac{0.6313}{t} \text{ mol dm}^{-3} \text{ s}^{-2} \quad (8)$$

Table 4-1 shows flux values obtained using $j_A = \frac{V_B}{A} \frac{dC_B}{dt}$.

Table 4-1: Flux values for Nafion[®] 117 membrane at various time periods for 2.5M initial methanol concentration

Time (s)	$\frac{dC_B}{dt} * 10^{-5} \text{ mol dm}^{-3} \text{ s}^{-2}$	$j_A * 10^{-6} \text{ mol cm}^{-2} \text{ s}^{-1}$
8060	7.83251	1.24415
9260	6.81749	1.08292
11120	5.67716	0.901787
13760	4.58794	0.72877
16820	3.75327	0.596187
18620	3.39044	0.538554

$$j_{A_{avg}} = \frac{\int_{t_i}^{t_f} j_A dt}{\int_{t_i}^{t_f} dt} \quad (9)$$

This implies that;

$$j_{A_{avg}} = \frac{\frac{0.6313 \text{ mol dm}^{-3} \text{ s}^{-2} * V_B}{A} \int_{t_i}^{t_f} \frac{1}{t} dt}{t_f - t_i}$$

$$j_{A_{avg}} = 48 \mu\text{mol cm}^{-2} \text{ min}^{-1}$$

And using equation (3), Permeability (DK) = $1.13 \times 10^{-6} \text{ cm}^2 \text{ s}^{-1}$

A comparison of the permeability values obtained in the present studies with literature values is given in Table 4-2.

Table 4-2: Nafion[®] Membrane Methanol Permeability

Author	Technique	Temperature °C	Methanol Conc. (M)	Permeability $\text{cm}^2 \text{s}^{-1} * 10^{-6}$
Present studies	Cyclic Voltammetry	22	2.5	1.27
Present studies	Chronoamperometry	22	2.5	1.11
Present studies	Potentiometry at OCV	22	2.5	1.13
Ramya et al	Cyclic Voltammetry and Chronoamperometry	30	2	5.3
Barragan et al	Open Circuit Voltage (OCV)	120	5	15.6
Tricoli et al	Gas chromatography	22	2	1.15

The cyclic voltammetry, chronoamperometry, and potentiometric techniques evaluated gave accurate permeability values. However, potentiometric technique has additional

advantages of giving more data points, and is more reliable because it allows easier reproducibility of results. In addition to these, is more convenient because the readings are automatically recorded by the potentiostat without necessarily having to stay and take the readings hourly. Thus, potentiometric technique has been chosen to be the best among the techniques evaluated. It was used to determine the methanol crossover flux in the prepared composite membranes.

4.2 SPEEK/TPA/ MCM-41 or Y-zeolite Composite Membranes Preparation

Both the methanol permeability and proton conductivity values of SPEEK membranes are low compared to that of Nafion[®] membranes. While incorporation of heteropolyacids into the SPEEK polymer matrix enhances the membranes proton conductivity, it also promotes methanol permeation through the membranes. In order to control the membranes methanol permeability, appropriate quantities of inorganic components such as ZrO₂, MCM-41, Y-zeolite etc, could be blended in the membranes.

SPEEK/TPA/Y-zeolite or MCM-41 composite membranes were prepared using the procedure described in section 3.2. During the preparation, it was observed that appropriate viscosity of the SPEEK/TPA/Y-zeolite or MCM-41 mixture before casting and flatness of the glass plate are very important in achieving homogeneous and uniform thickness membranes. Also, as the amount of the TPA/Y-zeolite or MCM-41 was increased up to 30wt % to 40wt % the membranes become fragile and brittle. This is expected because the inorganic component materials are not as flexible as the polymer matrix.

4.3 Methanol Permeability of SPEEK/TPA/ MCM-41 Composite Membranes

Having established that potentiometric technique is the best in terms of reliability and convenience; it was then used to study the methanol crossover behavior of the prepared composite membranes. Figure 4-15, shows potentiometric curves for pure SPEEK 1.6 membrane and three different composite membranes; 10wt % (50% MCM-41 + 50wt % TPA) and 90wt % SPEEK 1.6, 20wt % (50wt % MCM-41 + 50wt % TPA) and 80wt % SPEEK 1.6, and 30wt % (50wt % MCM-41 + 50wt % TPA) and 70wt % SPEEK 1.6, when 2.5M initial concentration was used in the reservoir compartment . It can be observed that as the inorganic loadings (MCM-41/TPA) increase from 10wt % to 30wt %, the potential values decrease. All the composite membranes have higher potential values compared to the pure SPEEK 1.6 membrane. These potential values were recorded and converted to concentrations using the calibration curve. The concentration values were used in determining the methanol crossover flux and the permeability of the membranes. Figure 4-16 shows an increase in methanol concentration in the receiving compartment with respect to time when 30wt % (50wt %MCM-41 + 50wt % TPA) and 70wt % SPEEK composite membrane was studied.

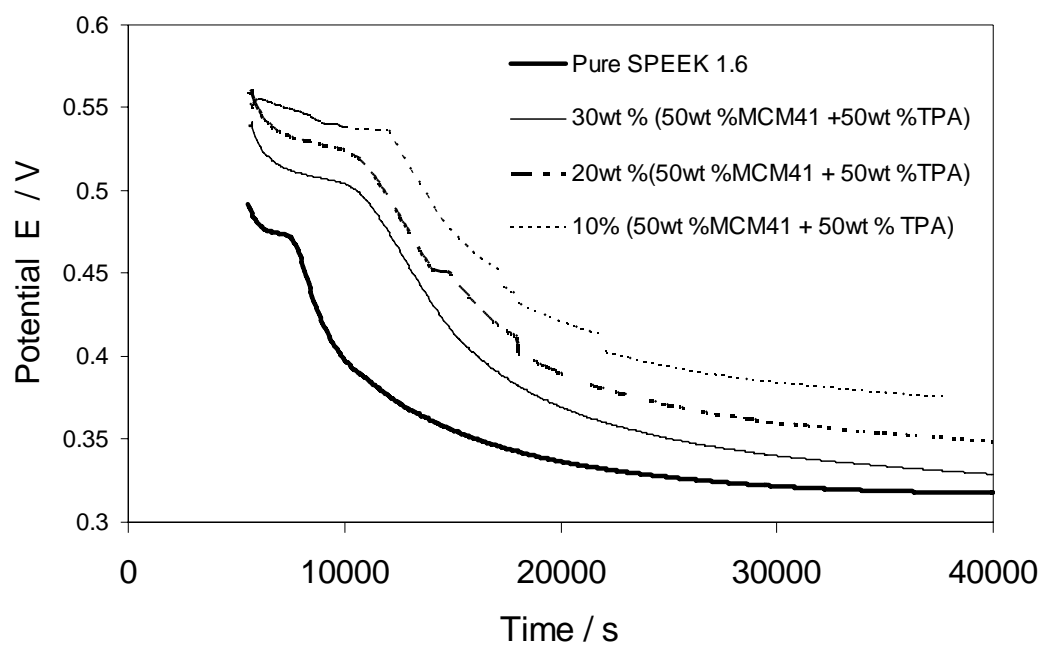


Figure 4-15: Potentiometric curves for pure SPEEK 1.6 membrane and three different SPEEK/TPA/MCM-41 composite membranes.

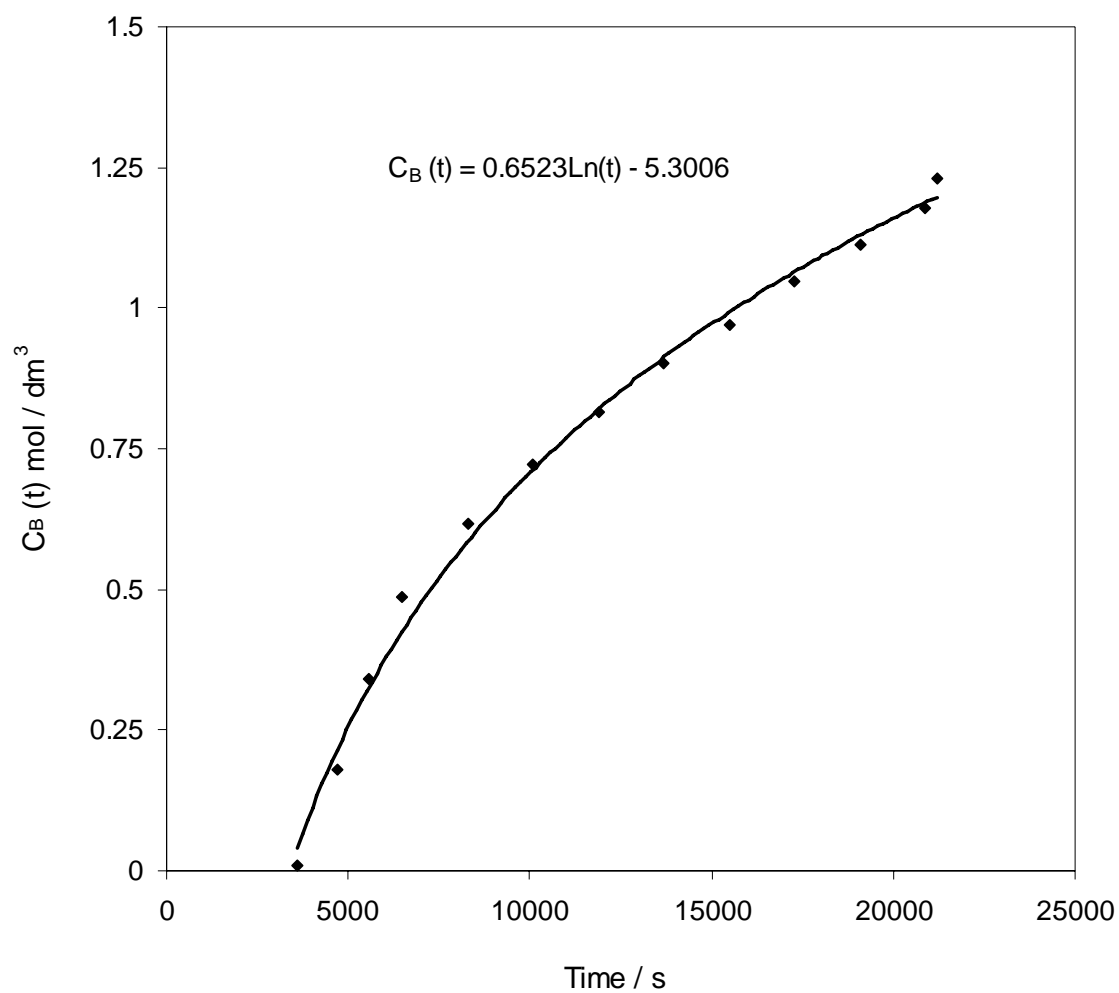


Figure 4-16: Variation in methanol concentration in the receiving compartment for 30wt % (50wt %MCM-41 + 50wt % TPA) and 70wt % SPEEK composite membrane for 2.5M initial methanol concentration in the reservoir compartment.

$$C_B(t) = 0.6523 * \ln(t) - 5.3006 \quad (1)$$

which means;

$$\frac{dC_B}{dt} = \frac{0.6523}{t} \text{ mol dm}^{-3} \text{ s}^{-2} \quad (2)$$

Table 4-3 shows flux values obtained using $j_A = \frac{V_B}{A} \frac{dC_B}{dt}$.

Table 4-3: Flux values for 30wt % (50wt %MCM-41 and 50wt % TPA) and 70wt % SPEEK composite membrane at various times for 2.5M initial methanol concentration

<i>Time (s)</i>	<i>E (V)</i>	<i>C_B (t)</i> <i>mol dm⁻³</i>	<i>C_A (t)</i> <i>mol dm⁻³</i>	$\frac{dC_B}{dt} * 10^{-5}$ <i>mol dm⁻³ s⁻²</i>	<i>j_A * 10⁻⁶</i> <i>mol cm⁻² s⁻¹</i>
3600	0.4954	0.0094	2.4906	18.1194	2.8782
4680	0.4870	0.1783	2.3217	13.9380	2.2140
5580	0.4789	0.3411	2.1589	11.6900	1.8569
6480	0.4717	0.4859	2.0141	10.0664	1.5989
8280	0.4652	0.6166	1.8834	7.8780	1.2514
10080	0.4600	0.7211	1.7789	6.4712	1.0279
11880	0.4554	0.8136	1.6864	5.4907	0.8722
13680	0.4510	0.9021	1.5979	4.7683	0.7574
15480	0.4476	0.9705	1.5295	4.2138	0.6693
17280	0.4437	1.0489	1.4511	3.7749	0.5996
19080	0.4406	1.1112	1.3888	3.4188	0.5431
20880	0.4373	1.1775	1.3225	3.1240	0.4962
21200	0.4371	1.2298	1.2702	3.0769	0.4887

$$j_{A_{avg}} = \frac{\int_{t_i}^{t_f} j_A dt}{\int_{t_i}^{t_f} dt} \quad (3)$$

This implies that;

$$j_{A_{avg}} = 62.63 \mu mol \text{ cm}^{-2} \text{ min}^{-1}$$

And using equation (3), Permeability (DK) = $3.506 \times 10^{-8} \text{ cm}^2 \text{ s}^{-1}$

The same procedure was followed to calculate the methanol crossover flux and diffusivity values for the other composite membranes.

Figure 4-17 shows an increase in methanol concentration in the receiving compartment with respect to time for pure SPEEK 1.6 membrane and four different composite membranes; 30wt % MCM-41 and 70wt % SPEEK 1.6, 10wt % (50% MCM-41 + 50wt % TPA) and 90wt % SPEEK 1.6, 20wt % (50wt % MCM-41 + 50wt % TPA) and 80wt % SPEEK 1.6, and 30wt % (50wt % MCM-41 + 50wt % TPA) and 70wt % SPEEK 1.6, when 2.5M initial concentration was used in the reservoir compartment.

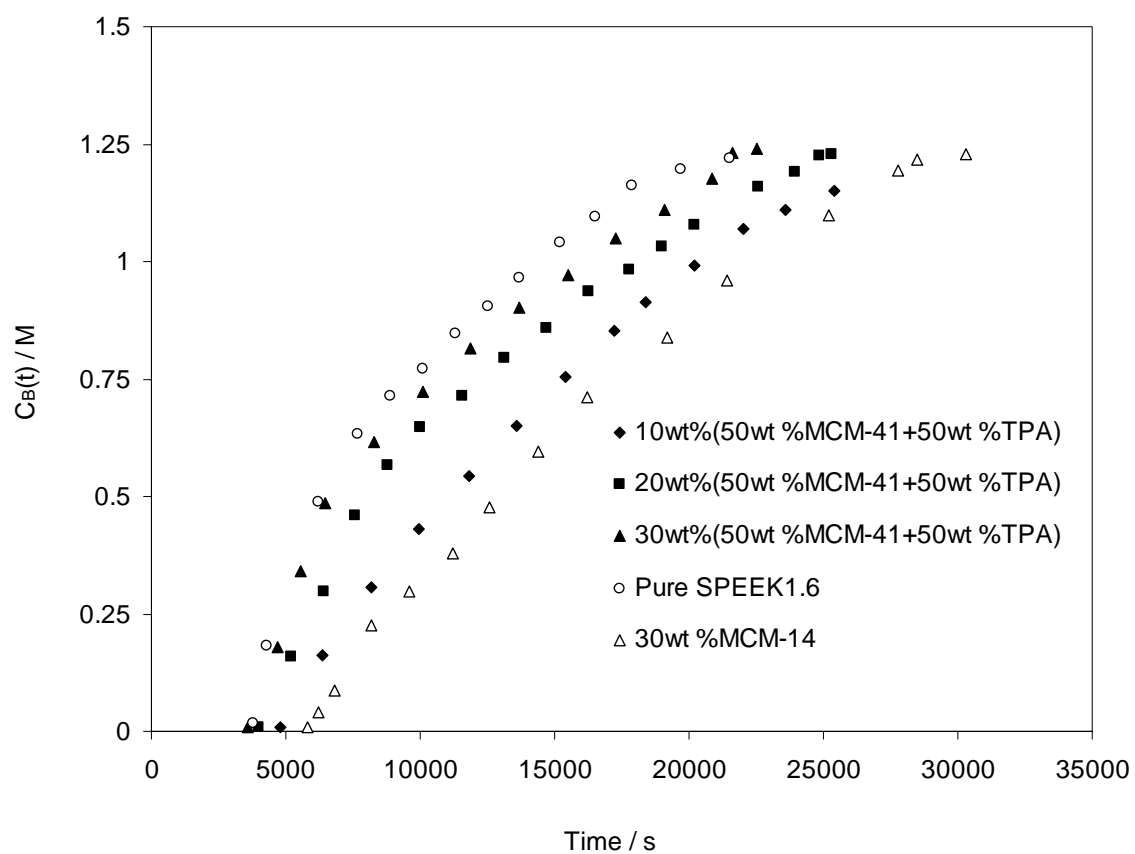


Figure 4-17: Variation in methanol concentration in the receiving compartment for pure SPEEK 1.6 membrane and the SPEEK/MCM-41/TPA composite membranes for 2.5M initial methanol concentration in the reservoir compartment.

The concentration values were used in determining the methanol crossover flux and permeability values for the membranes. Figure 4-18 shows a decrease in the flux values due to decrease in the concentration gradient during the crossover for the same membranes. It can be observed that as the amount of the inorganic loading increases the methanol crossover flux increases. That is, as the amount of the tungstophosphoric acid (TPA) which is known to enhance methanol permeation is increased the composite membranes become more permeable to the methanol. The presence of MCM-41 suppose to counter this TPA behavior but it was observed that when the MCM-41 weight percent is high its ability to suppress the effect of increasing methanol crossover caused by the TPA declines. Similar observation has been reported; silicates incorporated into polymer membranes help to reduce methanol permeability but at high loadings this contribution to reduction in methanol permeability is small [41]. Also, as the inorganic loadings increase, the membranes become more inhomogeneous, thus, creating voids through which permeation of methanol molecules could occur.

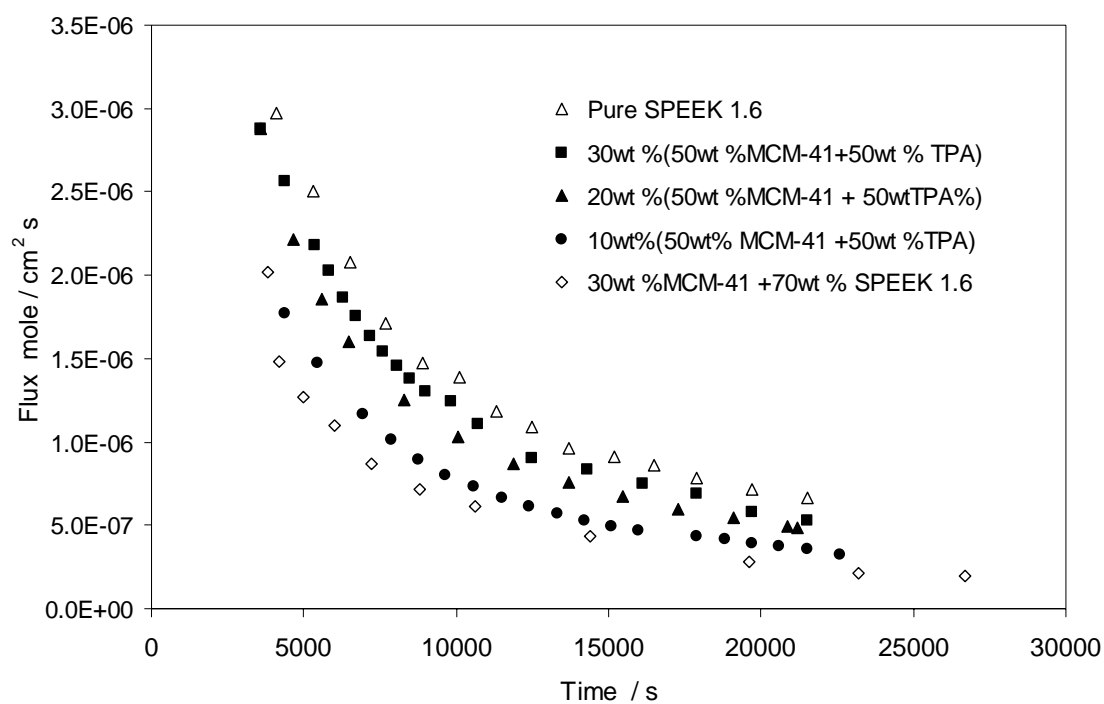


Figure 4-18: Methanol crossover flux for the pure SPEEK 1.6 membrane and the SPEEK/MCM-41/TPA composite membranes for 2.5M initial methanol concentration in the reservoir compartment.

However, even composite membrane with the highest inorganic loading (30wt %) has lower average methanol crossover flux and Permeability values compared to the plain SPEEK 1.6 as shown in Table 4-4.

Table 4-4: SPEEK/TPA/MCM-41 Membranes Permeability and Flux Values.

Membrane Type	Thickness (μm)	Permeability $\times 10^{-8}$ $cm^2 s^{-1}$	Average Flux $\left(\mu mol \right)$ $\left(cm^{-2} min^{-1} \right)$
Pure SPEEK 1.6	160	4.41	69.72
30wt % TPA and 70wt % SPEEK 1.6	160	7.29	96.08
30wt % MCM-41 and 70wt % SPEEK 1.6	160	0.83	30.20
30wt % (50wt % MCM-41 +50wt % TPA) and 70wt % SPEEK 1.6	160	3.51	62.65
20wt % (50wt % MCM-41 + 50wt % TPA) and 80wt % SPEEK 1.6	160	1.50	43.50
10wt % (50wt % MCM-41 + 50wt % TPA) and 90wt % SPEEK 1.6	120	1.32	40.60
30wt % (60wt % MCM-41 + 40wt % TPA) and 70wt % SPEEK 1.6	160	1.63	55.70
20wt % (60wt % MCM-41 + 40wt % TPA) and 80wt % SPEEK 1.6	145	0.69	37.78
10wt % (60wt % MCM-41 + 40wt % TPA) and 90wt % SPEEK 1.6	145	0.57	33.7

The presence of TPA in the composite membranes enhances membrane hydrophilicity, resulting in gain in proton conductivity while MCM-41 inhibits methanol crossover, decreases bleeding out of the TPA and increases thermal stability of the membranes. Thus, these composite membranes could perform better than SPEEK 1.6 in the operation of DMFC.

4.4 Methanol Permeability of SPEEK/TPA/ Y-zeolite Composite Membranes

The Y-zeolite serves the same purpose of inhibiting methanol permeation, decreasing leaching of the TPA and increasing thermal stability like the MCM-41. Using the potentiometric technique, potential values were recorded for each of the composite membranes and were converted to concentrations. Figure 4-19, shows potentiometric curves for pure SPEEK 1.6 membrane and three different composite membranes; 10wt % (60wt % Y-zeolite + 40wt % TPA) and 90wt % SPEEK 1.6, 20wt % (60wt % Y-zeolite + 40wt % TPA) and 80wt % SPEEK 1.6, and 40wt % (60wt % Y-zeolite + 40wt % TPA) and 60wt % SPEEK 1.6, when 2.5M initial concentration was used in the reservoir compartment. All the composite membranes except 40wt % (60wt % Y-zeolite + 40wt % TPA) and 60wt % SPEEK 1.6 have higher potential values compared to the pure SPEEK 1.6 membrane. These potential values were recorded and converted to concentrations using the calibration curve.

Figure 4-20 shows an increase in methanol concentration in the receiving compartment with respect to time when 40wt % (60wt %Y-zeolite + 40wt % TPA) and 60wt % SPEEK composite membrane was studied.

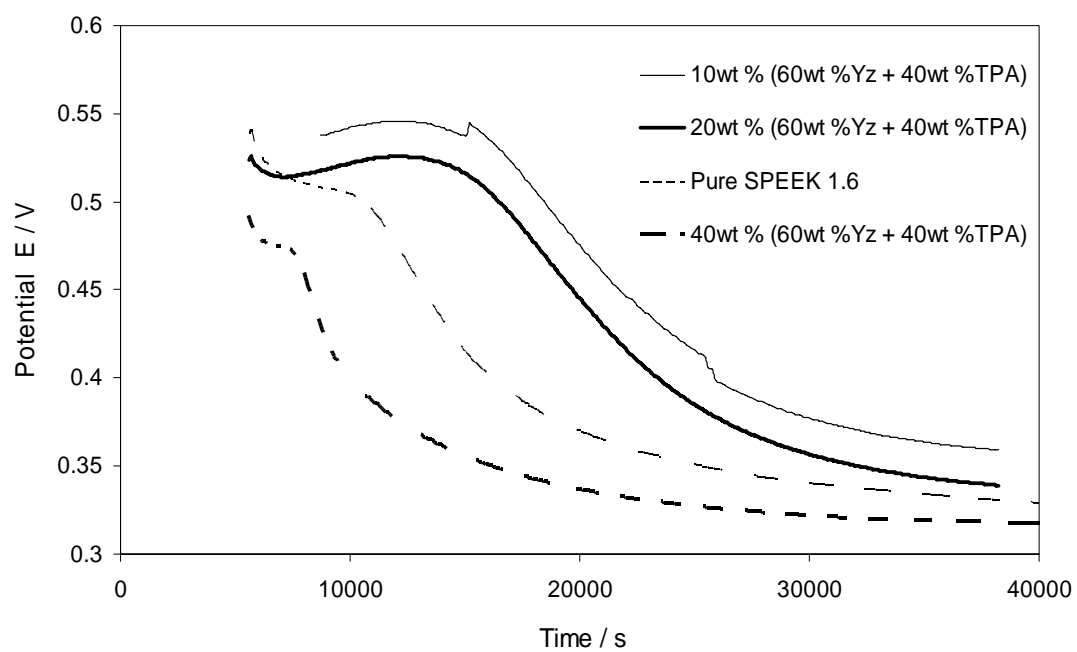


Figure 4-19: Potentiometric curves for pure SPEEK 1.6 membrane and three different SPEEK/TPA/Y-zeolite composite membranes.

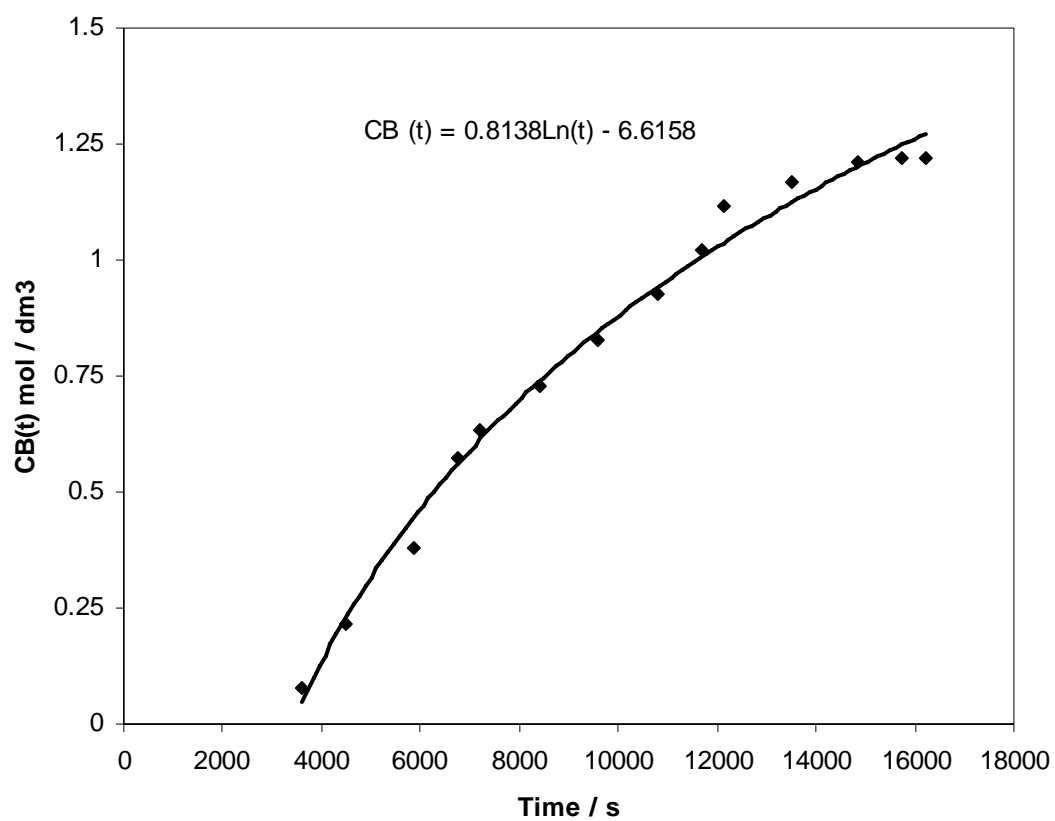


Figure 4-20: Variation in methanol concentration in the receiving compartment for 40wt % (60wt % Y-zeolite + 40wt % TPA) and 60wt % SPEEK composite membrane for 2.5M initial methanol concentration in the reservoir compartment.

From the plot;

$$C_B(t) = 0.8138 * \ln(t) - 6.6158 \quad (1)$$

This gives;

$$\frac{dC_B}{dt} = \frac{0.8138}{t} \text{ mol dm}^{-3} \text{ s}^{-2} \quad (2)$$

Table 4-5 shows flux values obtained using $j_A = \frac{V_B}{A} \frac{dC_B}{dt}$.

Table 4-5: Flux values for 40wt % (60wt %Y-zeolite and 40wt % TPA) and 60wt% SPEEK composite membrane at various times for 2.5M initial methanol concentration

<i>Time (s)</i>	<i>E (V)</i>	<i>C_B (t)</i> <i>mol dm⁻³</i>	<i>C_A (t)</i> <i>mol dm⁻³</i>	$\frac{dC_B}{dt} * 10^{-5}$ <i>mol dm⁻³ s⁻²</i>	<i>j_A * 10⁻⁶</i> <i>mol cm⁻² s⁻¹</i>
3600	0.4920	0.0775	2.4225	22.60	3.59
4500	0.4851	0.2165	2.2835	18.10	2.87
5850	0.4771	0.3773	2.1227	13.90	2.21
6750	0.4673	0.5744	1.9256	12.10	1.91
7200	0.4644	0.6327	1.8673	11.30	1.79
8400	0.4596	0.7292	1.7708	9.68	1.54
9600	0.4548	0.8257	1.6743	8.47	1.35
10800	0.4497	0.928	1.5718	7.53	1.20
11700	0.4450	1.0227	1.4773	6.95	1.10
12150	0.4404	1.1152	1.3848	6.69	1.06
13500	0.4378	1.1677	1.3323	6.03	0.96
14850	0.4357	1.2105	1.2895	5.48	0.87
16200	0.4352	1.22075	1.27925	5.02	0.80

$$j_{A_{avg}} = \frac{\int_{t_i}^{t_f} j_A dt}{\int_{t_i}^{t_f} dt} \quad (3)$$

This implies that;

$$j_{A_{avg}} = 92.5 \mu mol \text{ cm}^{-2} \text{ min}^{-1}$$

And using equation (3), Permeability (DK) = $7.04 \times 10^{-8} \text{ cm}^2 \text{ s}^{-1}$

Methanol crossover flux and permeability values for the other composite membranes were obtained using the same procedure. Figure 4-21 shows increase in methanol concentration in the receiving compartment with respect to time when 2.5M initial concentration was used in the reservoir compartment for pure SPEEK 1.6 membrane and four different SPEEK composite membranes; 30wt % Y-zeolite and 70wt % SPEEK 1.6, 20wt % (60wt % Y-zeolite + 40wt % TPA) and 80wt % SPEEK 1.6, 30wt % (60wt % Y-zeolite + 40wt % TPA) and 70wt % SPEEK 1.6, and 40wt % (60wt % Y-zeolite + 40wt % TPA) and 60wt % SPEEK 1.6. Figure 4-22 shows decrease in the flux values due to decrease in the concentration gradient during the crossover for the same membranes. It can be observed that as the amount of the inorganic loading increases and that of SPEEK 1.6 decreases the methanol crossover flux increases.

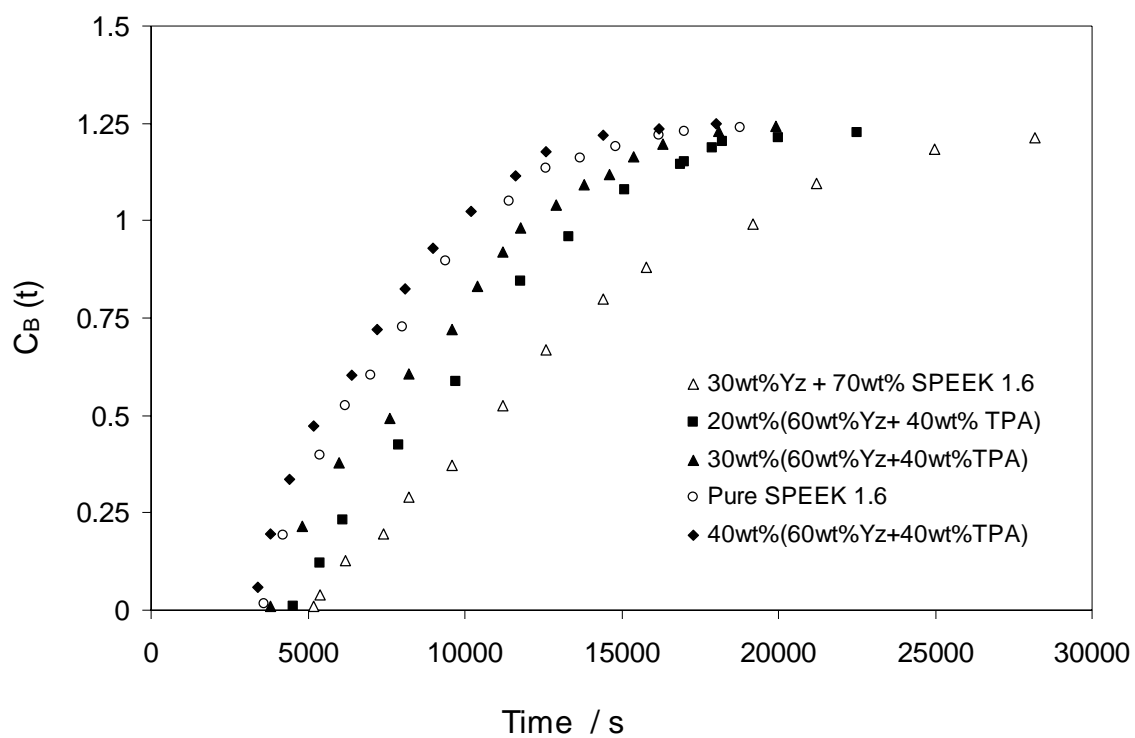


Figure 4-21: Variation in methanol concentration in the receiving compartment for the pure SPEEK 1.6 membrane and the SPEEK/Y-zeolite/TPA composite membranes for 2.5M initial concentration in the reservoir compartment.

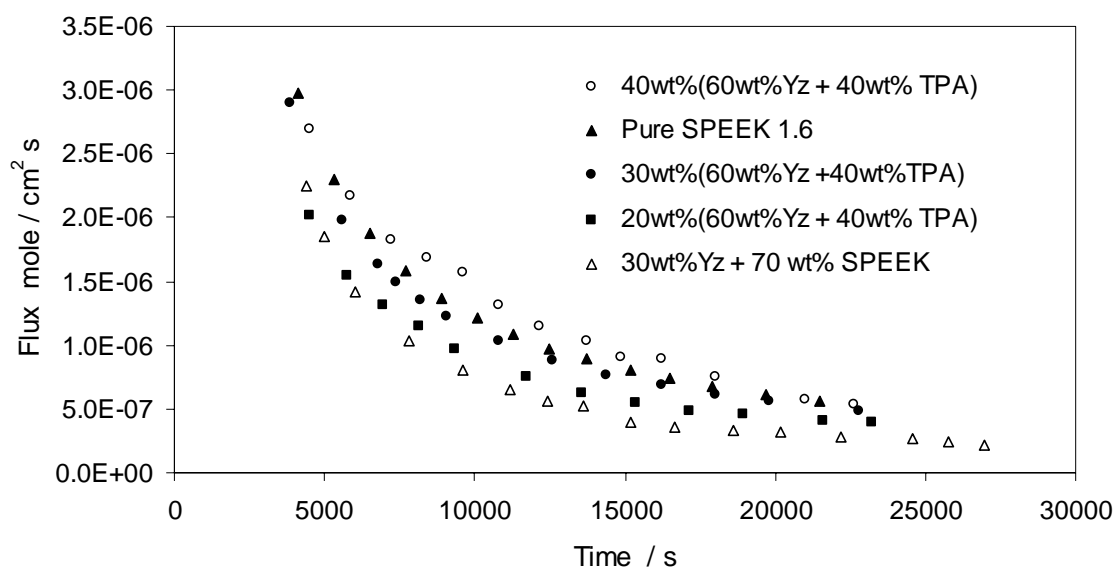


Figure 4-22: Methanol crossover flux for the pure SPEEK 1.6 membrane and the SPEEK/Y-zeolite/TPA composite membranes for 2.5M initial methanol concentration in the reservoir compartment.

It can be observed, that with lower inorganic loadings better reduction of methanol crossover flux is achieved. Table 4-6 shows the average methanol crossover flux and permeability values for the SPEEK/TPA/Y-zeolite composite membranes.

Table 4-6: SPEEK/TPA/Y-zeolite Membranes Permeability and Flux Values

Membrane Type	Thickness (μm)	Permeability $\times 10^{-8}$ $cm^2 s^{-1}$	Average Flux $\left(\mu mol \right)$ $\left(cm^{-2} min^{-1} \right)$
Pure SPEEK 1.6	160	4.41	69.72
30wt % TPA and 70wt % SPEEK 1.6	160	7.29	96.08
30wt % Y-zeolite and 70wt % SPEEK 1.6	160	1.64	49.50
30wt % (50wt % Y-zeolite + 50wt % TPA) and 70wt % SPEEK 1.6	160	4.29	64.55
20wt % (50wt % Y-zeolite + 50wt % TPA) and 80wt % SPEEK 1.6	160	3.27	57.96
10wt % (50wt % Y-zeolite + 50wt % TPA) and 90wt % SPEEK 1.6	145	1.71	50.83
40wt % (60wt % Y-zeolite + 40wt % TPA) and 60wt % SPEEK 1.6	160	7.04	92.50
30wt % (60wt % Y-zeolite + 40wt % TPA) and 70wt % SPEEK 1.6	160	3.34	62.60
20wt % (60wt % Y-zeolite + 40wt % TPA) and 80wt % SPEEK 1.6	145	2.12	52.50

It can be seen that composite membranes with MCM-41 have lower average methanol crossover flux and permeability values than those with Y-zeolite. MCM-41 is a mesoporous material with pore diameter of 3.0 nm to 3.2 nm. The MCM-41 used has silicon to aluminum ratio of 15. Y-zeolite is a microporous material with pore diameter of about 0.74 nm and low silicon to aluminum ratio. Because the pore diameter of MCM-41 is bigger, it can accommodate the TPA molecules within its pores better. This means provision of better framework for the loading of TPA. In Y-zeolite, the pores have small diameter, thus some of the TPA molecules could be exposed to the surface. But TPA molecules could still be effectively encapsulated in the supercages of the zeolite when there are a moderate number of aluminum atoms in the framework of the zeolite, and cations which promote the formation of TPA precursors occupy the cation sites induced by these atoms [71].

In general, all the composite membranes studied except one, have lower average methanol crossover flux and permeability values than plain SPEEK 1.6 membrane. The presence of TPA in the composite membranes will enhance their proton conductivity while the MCM-41 and Y-zeolite will prevent leaching of the TPA, increase thermal stability of the membranes and inhibits methanol permeation. Thus, SPEEK/TPA/MCM-41 or Y-zeolite composite membranes prepared could have better performance in the operation of DMFC than plain SPEEK 1.6.

CHAPTER 5

5 CONCLUSIONS AND RECOMMENDATIONS

5.1 Conclusions

Based on the results of this research work, the following conclusions are made:

- 1) Five methanol crossover measurement techniques through polymer electrolyte membranes including both electrochemical and non electrochemical have been screened. It was found that the electrochemical techniques are more accurate, reliable and convenient.
- 2) Three electrochemical techniques were experimentally screened; cyclic voltammetry, chronoamperometry, and potentiometry. Among them, potentiometric technique has been found to be the best in terms of easier reproducibility of results, convenience and ability of getting more data points.
- 3) Potentiometric technique was used in determining the methanol crossover flux and permeability of the prepared SPEEK/TPA/MCM-41 and SPEEK/TPA/Y-zeolite composite membranes.

- 4) All the SPEEK/TPA/MCM-41 composite membranes studied have lower average methanol crossover flux and permeability values than the plain SPEEK 1.6 membrane.
- 5) All the SPEEK/TPA/Y-zeolite composite membranes studied except the one with 40 wt % (60wt %Y-zeolite + 40wt % TPA) and 60wt % SPEEK 1.6 have lower average methanol crossover flux and permeability values than plain SPEEK 1.6.
- 6) Lower loadings of the inorganic material (TPA/MCM-41 or Y-zeolite) gives better reduction of methanol crossover than high loadings.
- 7) Composite membranes with MCM-41 showed lower average methanol crossover flux and permeability values than those with Y-zeolite.
- 8) The SPEEK/TPA/MCM-41 or Y-zeolite composite membranes studied have good potential for use in the direct methanol fuel cell (DMFC) due to their low methanol permeability.

5.2 Recommendations

The following recommendations could be useful for future studies,

- 1) More of the methanol crossover measurement techniques should be studied in order to make a more comprehensive conclusion on the best one (s).
- 2) Effects of temperature on the methanol permeability of the SPEEK/TPA/MCM-41 or Y-zeolite composite membranes should be studied.
- 3) The membranes should be tested in a direct methanol fuel cell (DMFC).

REFERENCES

1. Barbie, F., "PEM Fuel Cells: Theory and Practice", *Elsevier Inc.*, 2005.
2. Baldauf, M., Preidel, W., "Status of the development of direct methanol fuel cell", *Journal of Power Sources* 84 (1999) 161.
3. Hammet, A., *Philos. Trans. R. Soc. London*, A 354 (1996) 1653.
4. Narayanan, S. R., Kindler, A., Jeffries-Nakamura, B., Chun, W., Frank, H., Smart, M., Valdez, T. I., Surampudi, S., Halpert, G., Kosek, J., and Creply, C. , *Proceedings of 11th Annual Battery Conference Applied Advances*, 113 (1996).
5. Handbook of Fuel Cells "Fundamental Technology and Applications", *John Wiley*, Vol. 1, 2003.
6. Irfan, M. A., "Synthesis and Characterization of Composite Polymeric Membranes for Proton Exchange Membrane (PEM) Fuel Cell Applications", *M.S Thesis*, March 2005.
7. Kordesch, K., Simader, G., "Fuel Cell and Their Applications", *VCH Publishers Inc.*, New York, 1996, pp 151.
8. Handbook of Fuel Cells, "Fundamental Technology and Applications", *John Wiley*, vol. 4, 2003.
9. Li, S., Liu, M., "Synthesis and Conductivity of Proton Electrolyte Membranes Based on Hybrid Inorganic-Organic Copolymers", *Electrochimica Acta* 48 (2003) 4271-4276.
10. Li, L., Wang, Z. Y., "Sulfonated Poly (ether ether ketone) Membranes for Direct Methanol Fuel Cell", *Journal of Membrane Science* 226 (2003) 159-167.
11. Smitha, B., Sridhar, S., Khan, A. A., "Solid Polymer Electrolyte Membranes for Fuel Cell Applications – a review, *Journal of Membrane Science* (2005).

12. Xu, F., Innocent, C., Bonnet, B., Jones, D.J, Roziere, J., “Chemical Modification of Perfluorosulfonated Membranes with Pyrrole for Fuel Cell Application: Preparation, Characterization and Methanol Transport, *Fuel Cells* 5(3) (2005) 398 – 405.
13. Smith, M. A., Ocampo, A. L., Espinosa-Medina, M. A., Sebastian, P.J., “A Modified Nafion Membrane with in situ Polymerized Polypyrrole for the Direct Methanol Fuel Cell”, *Journal of Power Sources* 124(2003) 59 – 64.
14. Byungchan, B., Yong, H. H, Dukjoon, K., “ Preparation and Characterization of Nafion/poly (1-vinylimidazole) Composite Membrane for Direct Methanol Fuel Cell Application “, *Journal of the Electrochemical Society* 152(7) (2005) A1366 – A1372.
15. Jin, L., Huanting, W., Shaoan, C., Kwong-YU, C., “Nafion – Polyfurfuryl Alcohol Nanocomposite Membranes for Direct Methanol Fuel Cells”, *Journal of Membrane Science* 246(1) (2005) 95 – 101.
16. Hong, W., Yuxin, W., Shichang, W., “Study on the Preparation and Properties of PVdF – based – blend Nafion Membranes, *Gaofenzi Xuebao* 4(2002) 540 – 543.
17. Zhi-Gang, S., Xin, W., I-Ming, H., “Composite Nafion / Polyvinyl Alcohol Membranes for the Direct Methanol Fuel Cells”, *Journal of Membrane Science* 210(1) (2002), 147 – 153.
18. Jiang, R., Kunz, H. R., Fenton, J. M., “Improvement of DMFC Performance and Stability Using Multi – Layer Structure Membranes”, *230th ACS National Meeting*, Washington DC, August (2005).
19. Suzhen, R., Chennan, L., Xinsheng, Z., Zhimo, W., Suli, W., Gongquan, S., Qin, X., Xuefeng, Y., “Surface Modification of Sulfonated Poly (ether ether ketone) Membranes

- Using Nafion Solution for Direct Methanol Fuel Cells”, *Journal of Membrane Science* (2005), 247 (1-2), 59 – 63.
20. Baradie, B., Dodelet, J. P., Guay, P., “Hybrid Nafion ® Inorganic Membrane with Potential Applications for Polymer Electrolyte Fuel Cells”, *Journal of Electroanalytical Chemistry*, 489(1998) 209 – 214.
21. Weilin, Tianhong, X., L., Changpeng, L., Wei, X., “Low Methanol Permeable Composite Nafion/Silica/PWA Membranes for Low Temperature Direct Methanol Fuel Cells”, *Electrochimica Acta* 50 (16-17), (2005), 3280 – 3285.
22. Miyake, N., Wainright, J. S., Savinell, R. F., Ernest, B. Y., “Evaluation of a Sol-gel Derived Nafion/Silica Hybrid Membrane for Polymer Electrolyte Membrane Fuel Cell Applications 11. Methanol Uptake and Methanol Permeability”, *Journal of the Electrochemical Society* 148 (8), (2001), A909.
23. Dimitrova, P., Friedrich, K. A., Stimming, U., Vogt, B., “Modified Nafion ® - based Membranes for use in Direct Methanol Fuel Cells”, *Solid State Ionics* 150 (2002) 115 – 122.
24. Kim, D. W., Choi, H-S., Lee, C., Blumstein, A., Kang, Y., “Investigation on Methanol Permeability of Nafion Modified by Self – Assembled Clay – Nanocomposite Membrane for DMFC”, *Solid State Ionics* 176(11 – 12), (2005), 1079 – 1089.
25. Kim, Y-M., Park, K-W., Choi, J-H., Park, I. S., Sung, Y-E., “A Pd-impregnated Nanocomposite Nafion Membrane for use in High – Concentration Methanol Fuel in DMFC”, *Electrochemistry Communications* 5(2003) 571 – 574.

26. Xu, H., Kunz, H. R., Fenton, J. M., “Palladium Deposition on Proton Exchange Membranes for Direct Methanol Fuel Cells”, *American Chemical Society, Division of Fuel Chemistry* 50(2) (2005) 482 – 483.
27. Hai, S., Gongquan, S., Suli, W., Jianguo, L., Xinsheng, Z., Gouxian, W., Hengyoung, X., Shoufu, H., QIN, X., “Pd Electroless Plated Nafion Membrane for High Concentration DMFCs”, *Journal of membrane science* 259(1 – 2) (2005) 27 – 33.
28. Haolin, T., Sanping, P. M. j., Zhaohui, W., Runzhang, Y., “Self-Assembling Multi-Layer Pd Nanoparticles onto Nafion Membrane to Reduce Methanol Crossover”, *Colloids and Surfaces, A: Physicochemical and engineering aspects* 262(1 – 3) (2005) 65 – 70..
29. Prabhuram, J., Zhao, T. S., Liang, Z. X., Yang, H., Wong, C.W., “Pd and Pd-Cu Alloy Deposited Nafion Membranes for Reduction of Methanol Crossover in Direct Methanol Fuel Cells”, *Journal of the Electrochemical Society*, 152(7) (2005) A1390 – A1397.
30. Hejze, T., Gollas, B. R., Sauerbreg, R. K., Schmied, M., Hofer, F., Besenhard, J. O., “Preparation of Pd-coated Polymer Electrolyte Membranes and Their Application in Direct Methanol Fuel Cells”, *Journal of Power Sources* 140(1) (2005) 21 – 27.
31. Park, Y-S., Yamazaki, Y., “Low Methanol Permeable and high Proton-conducting Nafion/Calcium Phosphate Composite Membrane for DMFC”, *Solid State Ionics*, 176 (11-12), (2005), 1097 – 1089.
32. Gierke, T. D., Munn, G. E., Wilson, F. C., *Journal of Polymer Science; Polymer Physics Education*, 19(1981), 1687.

33. Krever, K. D., "On the Development of Proton Conducting Polymer Membranes for Hydrogen and Methanol Fuel Cells", *Journal of Membrane Science*, 185(2001), 29-39.
34. Li, L., Zhang, W., Wang, Y., "Sulfonated Poly (Ether Ether Ketone) Membranes for Direct Methanol Fuel Cell", *Journal of Membrane Science* 226(2003) 159-167.
35. Maria, G., Xiangling, J., Xianfeng, L., Hui, N., Hampsey, J. E., Yunfeng, L., "Direct Synthesis of Sulfonated Aromatic Poly (Ether Ether Ketone) Proton Exchange Membranes for Fuel Cell Applications", *Journal of Membrane Science* 234(1-2), (2004), 75-81.
36. Hui, L., Chengji, Z., Zhe, W., Wei, X., Hub, N., Alan, G., "Preparation and Characterization of Sulfonated Poly (Ether Ether Ketone) Proton Exchange Membranes for Fuel Cell Application", *Journal of Membrane Science*, 255(1-2), (2005), 149-155.
37. Vetter, S., Ruffmann, B., Buder, I., Nunes, S.P., "Proton Conducting Membranes for Sulfonated Poly (Ether Ketone Ketone)", *Journal of Membrane Science*, 260(1-2), (2005), 181-186.
38. Zaidi, S. M. J., Mikhailenko, S.D., Robertson, G.P., Guiver, M.D., Kaliaguine, S., "Proton Conducting Composite Membranes from Polyether Ether Ketone and Heteropolyacids for Fuel Cell Applications", *Journal of Membrane Science* 173 (2000), 17-34.
39. Ponce, M. L., Prado, L., Ruffmann, B., Richau, K., Mohr, R., Nunes, S.P., "Reduction of Methanol Permeability in Polyetherketone-heteropoly acid Membranes", *Journal of Membrane Science*, 217(1-2), (2003), 5-15.

40. Chang, J.H., Park, J. H., Park, G-G., Kim, C-S., Park, O-Ok., “Proton-Conducting Composite Membranes Derived From Sulfonated Hydrocarbon and Inorganic Materials”, *Journal of Power Sources* 124(2003), 18-25.
41. Mikhailenko, S.D., Zaidi, S. M. J., Kaliaguine, S., “Sulfonated Polyether Ether Ketone Based Composite Polymer Electrolyte Membranes”, *Catalysis Today* 67(2001), 225- 236.
42. Carretta, N., Tricoli, V., Picchionni, F., “Ionomeric Membranes Based on Partially Sulfonated Poly (Styrene): Synthesis, Proton Conduction and Methanol Permeation”, *Journal of Membrane Science* 166(2000), 189-197.
43. Shin, J-P., Chang, B-J., Kim, J-H., Lee, S-B., Suh, D. H., “Sulfonated Polystyrene/Composite Membranes”, *Journal of Membrane Science* 251(2005), 247-254.
44. Navarra, M. A., Materazzi, S., Panero, S., Scrosati, B., “PVdF-Based Membranes for DMFC Applications”, *Journal of the Electrochemical Society* 150(11), (2003), A1528-A1532.
45. Ren, S., Sun, C., Li , Z., Jin, W., Chen, W., Xin, Q., Yang, X., “Sulfonated Poly (ether ether ketone) / Polyvinylidene Fluoride Polymer blends for Direct Methanol Fuel Cells”, *Materials Letters* 60 (2006), 44-47.
46. Prakash, G. K., Smart, M. C., Wang, Q-J., Atti, A., Pleyne, V., Yang, B., McGrath, K., Alla, G. A., Narayanan, S. R., Chum, W., Valdez, T., Surampudi, S., Donald, P., Kathrine, B. L., “High Efficiency Direct Methanol Fuel Cell Based on Poly / Styrenesulfonic acid (PSSA) – Poly vinylidene Fluoride (PVdF) Composite Membranes”, *Journal of Fluorine Chemistry* 125(8), (2004) 1217-1230.

47. Saarinen, V., Kallio, T., Paronan, M., Tikkanen, P., Rauhala, E., Kontturi, K., “New ETFE-based Membrane for Direct Methanol Fuel Cell”, *Electrochimica Acta* 50(2005) 3453-3460.
48. Shen, M., Roy, S., Kuhlmann, J. W., Scott, K., Lovell, K., Horsfall, J. A., “Grafted Polymer Electrolyte Membrane for Direct Methanol Fuel Cells”, *Journal of Membrane Science* 251(1-2) (2005), 12-1-130.
49. Lvov, S. N., Zhou, X. Y., Benning, L., Wei, X. J., Fedkin, M. V., Allcock, H. R., Hofmann, M. A., Cannon, A. M., Kellam, E. C., morfold, R. V., “Development of Proton Conducting Membranes for High Temperature Direct Methanol Fuel Cells”, *Proceedings of Symposium on Energy Engineering in the 21st Century*, Hong-Kong, 4 (2000), 1483-1488.
50. Carter, R., Wycisk, R., Yoo, H., Pintauro, P. N., “Blended Polyphosphazene/ Polyacrylonitrile Membranes for Direct Methanol Fuel Cells”, *Electrochemical and Solid State Letters* 5(9) (2002), A195-A197.
51. Libby, B., Smyrl, W. H., Cussler, E. L., “Polymer-Zeolite Composite Membranes for Direct Methanol Fuel Cells”, *AIChE Journal* 49(4) (2003), 991-1001.
52. Jung, I., Kim, D., Yun, Y., Chung, S., Lee, J., Tak, Y., “Electro-oxidation of Methanol Diffused through Proton Exchange Membrane on Pt Surface: Crossover Rate of Methanol”, *Electrochimica Acta*, 50 (2004) 607-610.
53. Qi, Z., Kaufman, A., “Open Circuit Voltage and Methanol Crossover in DMFCs”, *Journal of Power Sources* 110 (2002) 177-185.

54. Carmo, M., Paganin, V. A., Rosolen, J. M., Gonzacez, E. R., "Alternative Supports for the Preparation of Catalyst for Low Temperature Fuel Cells: The Use of Carbon Nanotubes", *Journal of Power Sources* 142(2005) 169-176.
55. Verbrugge, M. W., "Methanol Diffusion in Per-fluorinated Ion-exchange Membranes" *Journal of Electrochemical Society*, 136 (1989) 417.
56. Wang, J. T., Wasmus, S., Savinell, R. F., "Real-time Mass Spectrometric Study of the Methanol Crossover in a Direct Methanol Fuel Cell", *Journal of the Electrochemical Society*, 143 (1996) 1233.
57. Ren, X. M., Zelenay, P., Thomas, S., Darey, J., Gottesfeld, S., *Journal of Power Sources*, 86 (2000), 111.
58. Ren, X. M., Springer, T. E., Zawodzinski, T. A., Gottesfeld, S., "Methanol Transport Through Nafion Membranes Electro-osmotic Drag Effects on Potential Step Measurements", 147 (2) (2000), 466-474.
59. Dohle, H., Divisck, J., Merggel, J., Oetjen, H. F., Zingler, C., Stolten, D., "Recent Developments of the Measurement of the Methanol Permeation in a Direct Methanol Fuel Cell", *Journal of Power Sources*, 105 (2002), 274.
60. Jiang, R., Chu, D., "CO₂ Crossover through a Nafion Membrane in a Direct Methanol Fuel Cell", *Electrochemical and Solid-State Letters*, 5 (7) (2002), A156-A159.
61. Drake, J. A., Wilson, W., Killen, K., "Evaluation of the Experimental Model for Methanol Crossover in DMFCs", *Journal of the Electrochemical Society*, 151 (3) (2004), A413-A417.

62. Jiang, R., Chu, D., “Comparative Studies of Methanol Crossover and Cell Performance for a DMFC”, *Journal of the Electrochemical Society*, 151 (1) (2004), A64-A76.
63. Barragan, V. M., Heinzl, A., “Estimation of the Membrane Methanol Diffusion Coefficient from Open Circuit Voltage Measurements in a Direct Methanol Fuel Cell”, *Journal of Power Sources* 104 (2002), 66-72.
64. Schaffer, T., Hacker, V., Tschinder, T., Besenhand, J. O., Prenninger, P., “Introduction of an Improved Gas Chromatographic Analysis and Comparison of Methods to Determine Methanol Crossover in DMFCs”, *Journal of Power Sources*, 145 (2005), 188-198.
65. Kuver, A., Kim, P-K., “Comparative Study of Methanol Crossover across Electro-polymerized and Commercial Proton Exchange Membrane Electrolytes for the acid Direct Methanol Fuel Cell”, *Electrochimica Acta*, 43 (16-17) (1998), 2527-2535.
66. Ramya, K., Dhathathreyan, K. S., “Direct Methanol Fuel Cells: Determination of Fuel Crossover in a Polymer Electrolyte Membrane”, *Journal of Electroanalytical Chemistry*, 542 (2003), 109-115.
67. Umeda, M., Hatakeyama, Y., Mohamedi, M., Uchida, I., “Assessment of Methanol Crossover through a Nafion Membrane Using a Platinum Microdisc Electrode”, *Electrochemistry Communication*, 72 No.2 (2004).
68. Ling, J., Savadogo, O., “Comparison of Methanol Crossover among Four Types of Nafion Membranes”, *Journal of Electrochemical Society*, 151 (10) (2004), A1604-A1610.
69. Munichandraiah, N., McGrath, K., Prakash, G. K. S., Aniszfeld, R., Olah, G. A., “A Potentiometric Method of Monitoring Methanol Crossover Through Polymer Electrolyte

Membranes of Direct Methanol Fuel Cells”, *Journal of Power Sources*, 117 (2003), 98-101.

70. Walsh, F., “A First Course in Electrochemical Engineering”, *Electrochemical Consultancy (Romsey) Ltd*, 1993.

71. Mukai, S. R., Lin, L., Masuda, T., Hashimoto, K., “Key Factors for the Encapsulation of Keggin-type Heteropoly Acids in the Supercages of Y-type Zeolite”, *Chemical Engineering Science* 56 (2001) 799-804.

VITAE

Name	Mukhtar Bello
Religion	Islam
Nationality	Nigerian
Date of Birth	May 15, 1974
Permanent Address	Shiyar Jagwanawa, Yabo Yabo Local Government Sokoto State, Nigeria.
Education	Bachelor of Engineering (B.ENG) in Chemical Engineering Ahmadu Bello University, Zaria, Nigeria, February, 2000. Master of Science (MS) in Chemical Engineering King Fahd University of Petroleum & Minerals, Dhahran, Saudi Arabia, May 2006.
Research Interests	Chemical Reaction Engineering, Fuel Cells, and Environmental Pollution Control.